

Quark, lepton and right-handed neutrino production via inflation

Duarte Feiteira¹, Fotis Koutroulis^{2,3}, Oleg Lebedev¹ and Stefan Pokorski⁴

¹ *Department of Physics and Helsinki Institute of Physics,
Gustaf Hällströmin katu 2a, FI-00014 Helsinki, Finland*

² *Theoretical Physics Division, Institute of High Energy Physics, Chinese Academy of Sciences,
19B Yuquan Road, Shijingshan District, Beijing 100049, China*

³ *China Center of Advanced Science and Technology, Beijing 100190, China*

⁴ *Institute of Theoretical Physics, Faculty of Physics, University of Warsaw, Pasteura 5,
PL 02-093, Warsaw, Poland*

Abstract

Inflationary expansion of space-time provides us with an efficient particle production mechanism in the Early Universe. The fermion production efficiency depends critically on the particle mass, which is generated via the Yukawa coupling and sensitive to the corresponding scalar field value. During inflation, scalar fields experience large quantum fluctuations driving the average field values to the Hubble scale and above. This applies, in particular, to the Higgs field, making the Standard Model fermions very heavy and facilitating their production. Using the Bogolyubov coefficient approach, we compute the corresponding fermion abundance taking into account time dependence of the mass term. We find that the Standard Model fermion and the right-handed neutrino production grows dramatically compared to the naive estimate based on the low energy masses. The inflationary production mechanism can be the leading source of the right handed neutrinos, if they gain a Majorana mass from the Yukawa coupling to a light scalar. We also find a lower bound on the mass of fermionic dark matter, which can be produced by inflation.

Contents

1	Introduction	1
2	Basics of fermion production in an expanding Universe	3
3	Fermion production with a time-dependent mass: inflation followed by radiation domination	5
3.1	Fermion masses via Yukawa couplings: the Early Universe	6
3.2	Radiation dominated era	8
3.2.1	Step-function mass term	9
3.2.2	Slow effective mass decrease and thermal effects	14
4	Standard Model fermion and right-handed neutrino production via inflation	18
4.1	Quark and lepton production	18
4.1.1	Sharp effective mass decrease	18
4.1.2	Slow effective mass decrease	19
4.1.3	Top-quark production	20
4.1.4	No Higgs condensate	21
4.2	Inflationary production of the right-handed neutrinos due to the Higgs coupling .	21
4.2.1	Production of ν_R due to the background evolution	21
4.2.2	Direct neutrino production from the primordial Higgs condensate	22
4.2.3	Freeze-in ν_R production	23
4.3	Inflationary right-handed neutrino production due to the singlet scalar coupling .	23
4.3.1	Large N limit for fermion production	24
4.3.2	Upper bound on the abundance of gravitationally produced fermions . .	25
4.3.3	Feebly interacting scalar extension	25
5	Inflation followed by the matter dominated era	27
5.1	Constant mass	28
5.2	Step-function mass term	28
5.2.1	Universal form	30
6	Conclusion	31

1 Introduction

Particle production in the Early Universe plays an important role in modern cosmology [1]. First and foremost, it is responsible for reheating, that is, the inflaton energy conversion into the Standard Model (SM) quanta. This may be accompanied by production of dark matter (DM), either through its coupling to the SM states or via an independent mechanism. The latter possibility has been gaining traction due to the null direct DM detection results [2]. Dark matter production does not require significant couplings and it can even be produced via gravitational interactions.

Gravitational particle production [3]-[5] creates an irreducible background in any model of the Early Universe. This is particularly important in the context of non-thermal dark matter [6]. More generally, given that the specifics of reheating remain unknown, gravitational particle production can make an impact on the Early Universe composition and dynamics. In particular,

it is important to understand the efficiency of the SM particle production due to inflation [7]-[9] itself, which so far has not been accomplished in realistic settings.

In this work, we use the Bogolyubov coefficient approach [10] to study fermion production due to inflation, taking into account time dependence of the fermion masses. This applies, in particular, to the SM fermions whose masses are determined by the Higgs field value. During inflation, the Higgs field is driven to very large values, unless it has a significant positive coupling to the inflaton. Therefore, the fermions are expected to become heavy, which facilitates their gravitational production. It is known that the abundance (Y) of fermions produced via inflation scales with the (constant) fermion mass M as [11, 12]

$$Y \propto \left(\frac{M}{M_{\text{Pl}}} \right)^{3/2}, \quad (1)$$

assuming that inflation is followed by a radiation dominated epoch. The mass term breaks the conformal symmetry of the fermion action and, as such, plays the critical role in particle production. In contrast, the conformal symmetry is broken in the scalar sector already in the massless limit, unless the scalar has a specific non-minimal coupling to curvature. This breaking is communicated efficiently to the fermion sector via the Yukawa coupling, making the fermions very heavy in the Early Universe.

During inflation with Hubble rate H , a scalar field average value tends asymptotically to [13, 14]

$$\langle s^2 \rangle \rightarrow \frac{3H^4}{8\pi^2 m^2} \quad \text{or} \quad \sqrt{\frac{3}{2\pi^2}} \frac{\Gamma(3/4)}{\Gamma(1/4)} \frac{H^2}{\sqrt{\lambda}}, \quad (2)$$

depending on which term dominates the scalar potential. Here, $m \ll H$ is the scalar mass and λ is the self-coupling, $V(s) = \frac{1}{2}m^2 s^2 + \frac{1}{4}\lambda s^4$. Hence, unless the scalar is extremely heavy, it takes on a value of order H or above. Since inflation has a finite duration, the scalar may not reach its asymptotic value, yet its field value will be around H after 60 e-folds. When applied to the Higgs field, this makes the SM fermions up to 11 orders of magnitude heavier than they currently are, and increases dramatically the efficiency of their production.

The above scaling of the fermion abundance (1) only applies to a constant mass term and thus is inadequate for a realistic situation. The Higgs field value drops shortly after inflation, which introduces the fermion mass time-dependence. In this work, we compute the fermion abundance with a time-dependent mass using two Ansätze describing a sharp and a slow mass variation in the postinflationary period. Our results exhibit a different scaling behavior compared to that in (1).

Our considerations also apply to production of the right-handed neutrinos via inflation. These can potentially play the role of dark matter [15, 16], making the gravitational production channel particularly important. The large neutrino mass in the Early Universe can be generated either via the Higgs Yukawa coupling or a coupling to a singlet scalar, which produces a Majorana-type mass term. The latter turns out to be particularly interesting rendering the inflationary neutrino production efficient. We also derive the lower bound of about 10 GeV on the fermionic dark matter mass that can be produced by inflation. It is worth noting that our analysis is based on *classical* gravity and as such is well under control.

2 Basics of fermion production in an expanding Universe

Let us briefly summarize basics of fermion production in curved space-time [4]. Further details can be found in Refs. [11, 12]. Basics of gravitational particle production have been reviewed in [17, 18].

The Dirac equation in curved space reads

$$(i\gamma^\alpha \nabla_\alpha - M) \Psi = 0. \quad (3)$$

It follows from the action $\int d^4x \sqrt{|g|} \bar{\Psi} (i\gamma^\alpha \nabla_\alpha - M) \Psi$, where $g_{\mu\nu}$ is the space-time metric, ∇ is the covariant derivative and α is the local Lorentz index. The Friedmann metric in terms of the conformal time $x_0 \equiv \eta$ is given by

$$ds^2 = a(x_0)^2 \eta_{\mu\nu} dx^\mu dx^\nu. \quad (4)$$

With the help of the Weyl transformation

$$g_{\mu\nu} = \Omega^2 \tilde{g}_{\mu\nu}, \quad \Psi = \Omega^{-3/2} \tilde{\Psi}, \quad e_\alpha^\mu = \Omega^{-1} \tilde{e}_\alpha^\mu, \quad (5)$$

where $\Omega = a(x_0)$ and e_α^μ is the vierbein, $a(x_0)$ can be eliminated from the action, apart from the mass term. Dropping the tilde over the transformed quantities, the Dirac equation now reads

$$(i\gamma^\mu \partial_\mu - a(\eta)M) \Psi = 0. \quad (6)$$

It is the flat space Dirac equation with a time-dependent mass. In general, both $a(\eta)$ and M can evolve in time, leading to particle production.

The solution can be written in terms of the basis functions U_i, V_i with constant coefficients,

$$\Psi(x) = \sum_i \left(a_i U_i + b_i^\dagger V_i \right), \quad (7)$$

where i denotes collectively the spin and momentum indices. In the Heisenberg picture, a_i, b_i are operators with the usual time-independent anti-commutation relations, $\{a_i, a_j^\dagger\} = \delta_{ij}$, $\{b_i, b_j^\dagger\} = \delta_{ij}$, etc. The basis functions are given by

$$U_{\mathbf{k},s}(\eta, \mathbf{x}) = \frac{e^{i\mathbf{k}\cdot\mathbf{x}}}{(2\pi)^{3/2}} \begin{pmatrix} u_{A,k}(\eta) \\ s u_{B,k}(\eta) \end{pmatrix} \otimes h_s(\hat{\mathbf{k}}), \quad (8)$$

$$V_{\mathbf{k},s}(\eta, \mathbf{x}) = -\frac{e^{-i\mathbf{k}\cdot\mathbf{x}}}{(2\pi)^{3/2}} \begin{pmatrix} -u_{B,k}^*(\eta) \\ s u_{A,k}^*(\eta) \end{pmatrix} \otimes h_s(-\hat{\mathbf{k}}) e^{i\phi}, \quad (9)$$

where $k \equiv |\mathbf{k}|$, $\hat{\mathbf{k}} = \mathbf{k}/|\mathbf{k}| = (\theta, \phi)$ in spherical coordinates and h_s are the helicity 2-spinors satisfying

$$\hat{\mathbf{k}} \cdot \vec{\sigma} h_s = s h_s, \quad s = \pm 1, \quad (10)$$

with $\vec{\sigma}$ being the Pauli matrices. The gamma matrices are taken to be of the form

$$\gamma^0 = \begin{pmatrix} I & 0 \\ 0 & -I \end{pmatrix}, \quad \gamma^i = \begin{pmatrix} 0 & \sigma^i \\ -\sigma^i & 0 \end{pmatrix}. \quad (11)$$

The 2-spinors satisfy

$$h_s^\dagger(\hat{\mathbf{k}}) h_r(\hat{\mathbf{k}}) = \delta_{rs}, \quad (12)$$

such that requiring orthonormality of the basis

$$(U_i, U_j) = (V_i, V_j) = \delta_{ij} , \quad (U_i, V_j) = 0 , \quad (13)$$

leads to the condition

$$|u_A|^2 + |u_B|^2 = 1 . \quad (14)$$

Here $(f, g) = \int d^3x f^\dagger g$ and the spacial part of the wave functions is described by the orthonormal set $\frac{e^{i\mathbf{k}\cdot\mathbf{x}}}{(2\pi)^{3/2}}$.

The Dirac equation with the above Ansatz reduces to

$$i\partial_\eta \begin{pmatrix} u_A \\ u_B \end{pmatrix} = \begin{pmatrix} aM & k \\ k & -aM \end{pmatrix} \begin{pmatrix} u_A \\ u_B \end{pmatrix} . \quad (15)$$

It is to be solved with specific boundary conditions. The Bunch-Davies initial condition corresponds to the flat space vacuum $a_i|0\rangle = b_i|0\rangle = 0$ [19]. This defines the *in* wavefunction: at $\eta \rightarrow -\infty$, the $a(\eta)M$ terms become negligible and the positive frequency solution is

$$\begin{pmatrix} u_A \\ u_B \end{pmatrix}^{\text{in}} \xrightarrow{\eta \rightarrow -\infty} \begin{pmatrix} 1/\sqrt{2} \\ 1/\sqrt{2} \end{pmatrix} e^{-ik\eta} . \quad (16)$$

This determines $u_{A,B}$ uniquely.

Another “vacuum” can be defined in the infinite future by requiring no particles with respect to the corresponding number operator. At $\eta \rightarrow \infty$, the evolution matrix is diagonal and the positive eigenvalue solution corresponds to

$$\begin{pmatrix} u_A \\ u_B \end{pmatrix}^{\text{out}} \xrightarrow{\eta \rightarrow \infty} \begin{pmatrix} 1 \\ 0 \end{pmatrix} e^{-i \int \omega(\eta) d\eta} , \quad (17)$$

with $\omega \rightarrow a(\eta)M$. This asymptotic form, however, does not determine the normalization of u_B . To recover it, one expands the evolution matrix in $k/(aM)$ and finds that the relevant eigenvector contains $k/(2aM)$ instead of zero in the lower entry.

The solutions with different boundary conditions are related to each other linearly, with constant coefficients. Under the basis change,

$$\tilde{U}_{\mathbf{k},s} = \alpha_{\mathbf{k},s} U_{\mathbf{k},s} + \beta_{\mathbf{k},s} V_{-\mathbf{k},s} , \quad (18)$$

where the tilde refers to the quantity in the new basis. Since $\Psi(x)$ remains invariant, the basis change requires a linear redefinition of the creation and annihilation operators. Using the orthonormality condition, one finds the Bogolyubov coefficient

$$\beta_{\mathbf{k},s} = \text{phase} \times (u_{A,k} \tilde{u}_{B,k} - u_{B,k} \tilde{u}_{A,k}) , \quad (19)$$

where the time-independent phase is irrelevant for our purposes. Its importance lies in the property that it measures the particle number. Identifying the tilded/un-tilded objects with *out/in* quantities, one finds that $|\beta_i|^2$ corresponds to the average number of particles in the *in* vacuum $|0\rangle$ with respect to the *out* number operator,

$$\langle \tilde{N}_{\mathbf{k},s} \rangle \equiv \langle 0 | \tilde{a}_{\mathbf{k},s}^\dagger \tilde{a}_{\mathbf{k},s} | 0 \rangle = |\beta_{\mathbf{k},s}|^2 . \quad (20)$$

The physical number density is then

$$n = \sum_s \int \frac{d^3\mathbf{k}}{(2\pi)^3 a^3} |\beta_{\mathbf{k},s}|^2. \quad (21)$$

To compute the Bogolyubov coefficient, one finds the *in* and *out* solutions to the EOM and uses (19). The solutions are functions of time, while the Bogolyubov coefficient is constant and can be computed at any convenient point,

$$\beta'_{\mathbf{k},s} = 0, \quad (22)$$

where the prime stands for the η -derivative. For analytical estimates, one may choose $\eta \sim \eta_e$ corresponding to the end of inflation. At this point, both *in* and *out* solutions can be evaluated reliably.

The above considerations are also valid for a time-dependent mass $M = M(\eta)$ as long as it does not affect the $\eta \rightarrow \pm\infty$ boundary conditions. In the Standard Model, the fermion mass is determined by the average Higgs field value, which exhibits strong time dependence in the Early Universe. In particular, it is expected to be very large during and shortly after inflation, making fermion production much more efficient.

3 Fermion production with a time-dependent mass: inflation followed by radiation domination

The fermion mass in the Early Universe is determined by the environmental effects, e.g. the scalar field expectation value, and hence is time-dependent. Our starting point is the Dirac equation in curved space-time, where the mass term $M(\eta)$ can carry explicit time dependence controlled by the background evolution. Denoting the time derivative ∂_η by a prime, one may reduce the system (15) to the second order differential equations,

$$u_A'' + [i(Ma)' + a^2 M^2 + k^2] u_A = 0, \quad (23)$$

$$u_B'' + [-i(Ma)' + a^2 M^2 + k^2] u_B = 0, \quad (24)$$

where k is the magnitude of the 3-momentum. Compared to the constant mass case, this system contains an extra term proportional to $M'a$, which can have significant effects. For an abrupt mass variation, this term brings in a sharp feature, e.g. a delta-function. The wavefunction $u_{A,B}$ remains, however, smooth.

The solutions must have certain asymptotic behaviour corresponding to the *in* or *out* vacuum. At $a \rightarrow 0$ or $a \rightarrow \infty$, we recover approximately the flat space results with constant M , which are encoded in the definition of the *in* and *out* vacua. During inflation, the solutions with constant M are the Hankel functions of η , which also apply to an adiabatically changing $M(\eta)$. After inflation, the situation is more complicated and requires a detailed analysis. In what follows, we focus on “light” fermions in the sense $M(\eta) \ll H_e$, where H_e is the Hubble rate at the end of inflation.

Our goal is to compute the Bogolyubov coefficient at the end of inflation, $\eta \sim \eta_e$, where both the *in* and *out* solutions can be found analytically using reasonable approximations. We also calculate the Bogolyubov coefficient numerically, without resorting to approximations and using a smooth transition function $a(\eta)$ between inflation and the radiation domination era. Subsequently, we compute the particle density and the abundance.

We note that some aspects of inflationary fermion production have been studied in [20, 21], although in a different context. Postinflationary perturbative fermion production via graviton exchange was considered in [22], while general gravity-induced operators were analyzed in [12].

3.1 Fermion masses via Yukawa couplings: the Early Universe

In the Standard Model, gauge symmetry requires that the fermion masses M_f be generated via the Yukawa couplings $\frac{1}{\sqrt{2}} Y_f h \bar{f}_L f_R + \text{h.c.}$,

$$M_f = \frac{1}{\sqrt{2}} Y_f \langle h \rangle , \quad (25)$$

where h is the Higgs field in the unitary gauge and $\langle h \rangle$ is its expectation value. This also applies to the neutrinos, assuming that they have the right-handed counterparts ν_R ,

$$M_\nu^{\text{Dirac}} = \frac{1}{\sqrt{2}} Y_\nu \langle h \rangle . \quad (26)$$

In addition, the right-handed neutrinos may have a Majorana mass term $\frac{1}{2} \mathcal{M} \nu_R \nu_R + \text{h.c.}$, which could in turn be generated by an expectation value of an SM singlet s .

The central point of our work is that the Higgs field takes on a large value in the Early Universe¹, thereby making the SM fermion very heavy. This is required by the de Sitter fluctuations of the scalar fields and is independent of the inflationary model details. The Higgs field variance tends to the value [14]

$$\langle h^2 \rangle \rightarrow 0.1 \frac{H^2}{\sqrt{\lambda_h}} , \quad (27)$$

where λ_h is to be evaluated at the inflationary energy scale and we have neglected the bare mass term. This defines the long-wavelength average field, which can be treated as an effective “zero-mode” for our purposes. The above asymptotic value is reached rather quickly, on the timescale of $(\sqrt{\lambda_h} H)^{-1}$. Therefore, one may take

$$\langle h \rangle \simeq H_e \quad (28)$$

as the representative Higgs field value at the end of inflation. Here H_e is the corresponding Hubble rate and we have assumed $\lambda_h(H) \sim 10^{-2}$. One should keep in mind that the Higgs self-coupling at high energies is sensitive to the top-quark mass and thus is subject to substantial uncertainties, so the above value should not be taken as a precise prediction of the Standard Model.

This shows that the Standard Model fermions become heavy in the Early Universe, by up to 11 orders of magnitude. For the typical inflationary value $H_e \sim 10^{13}$ GeV, the bottom quark weighs as much as 10¹¹ GeV, while the top quark mass is similar to the Hubble rate. The neutrino mass can also be significant, up to 10 GeV, although the result depends on the unknown Yukawa couplings. In all cases of interest (apart from the top-quark),

$$M_f \ll H_e , \quad (29)$$

such that the fermions can be considered “light” in inflationary terms. The top-quark, however, requires a separate consideration.

¹This assumes the absence of significant (positive) Higgs couplings to the inflaton or the Ricci scalar R .

Gravitational particle production is sensitive to the fermion mass M . The fermion abundance produced by inflation itself is given by

$$Y_0 \simeq 5 \times 10^{-3} \left(\frac{M}{M_{\text{Pl}}} \right)^{3/2}, \quad (30)$$

assuming radiation-dominated postinflationary dynamics [11, 12]. Hence, for large $\langle h \rangle$ one expects much more efficient particle production than that based on the naive rigid fermion masses. This is particularly interesting for the right-handed neutrinos, which can potentially account for dark matter.

We note that particle production occurs due to conformal symmetry breaking. In the fermion case, the relevant symmetry breaking parameter is the fermion mass. Although this is a small parameter at low energies, it is driven to large values by the conformally-breaking scalar dynamics in the Early Universe. The latter is significant as long as the non-minimal coupling to gravity takes on a value different from 1/6. Hence, large symmetry breaking effects in the scalar sector feed into the fermion dynamics.

In reality, the Early Universe fermion masses are not constant and depend on the Higgs or other scalar field dynamics. Specifically, the Higgs field goes through the following stages:

- starting with arbitrary initial conditions, it reaches the value of order H_e during inflation
- remains constant after inflation until the Hubble rate decreases to the level of the effective Higgs mass
- starts oscillating in the quartic potential and decays into the SM radiation
- takes on the electroweak value v at late times

Thus, the fermion masses remain large for some time after inflation and then decrease to the standard values. The precise way the masses decrease depends on complicated non-perturbative dynamics. To capture its main features, we consider two extreme possibilities: an abrupt drop and a slow thermal-like mass evolution. Presumably, the realistic situation is in between the two.

On the other hand, the fermion mass dynamics during inflation is well understood: the mass term evolves adiabatically and reaches the terminal value within 10 Hubble times or so. In the distant past, $k/a \gg M_f$, such that the mass does not affect the initial Bunch-Davies state of the fermions². We therefore may approximate the fermion wave function at the late stages of inflation by that of a free fermion with fixed mass $M_f = \frac{1}{\sqrt{2}} Y_f \langle h \rangle$, where $\langle h \rangle \simeq H_e$.

To compute the particle abundance, we use a smooth transition function $a(\eta)$ from inflation to the radiation or matter dominated epochs. We neglect small oscillations of the scale factor induced by the inflaton oscillations around the minimum. These can, in principle, have a significant effect on particle production [24] which we estimate in Sec. 4.3.2. In the rest of the paper, we focus on the smoothed out or averaged version of the scale factor function. The corresponding Hubble rate evolution is shown schematically in Fig. 1.

²We may assume the Bunch-Davies fermion vacuum at the beginning of inflation. In contrast, for scalars, such an assumption would be inadequate due to possible existence of a significant scalar condensate with $k \simeq 0$ [23].

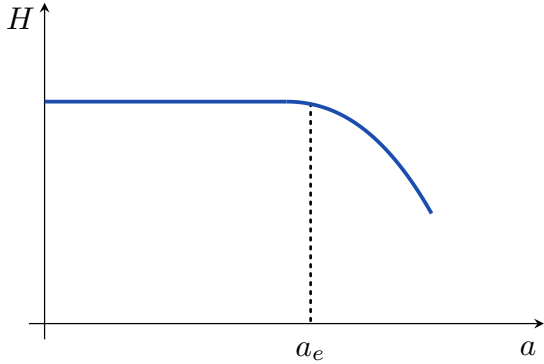


Figure 1: Hubble rate evolution assumed in this work. Inflation ends at $a \sim a_e$ and is followed by the radiation or matter domination epochs.

3.2 Radiation dominated era

Suppose that inflation is followed by the epoch, in which the equation of state of the Universe can be approximated by that of radiation. This can happen due to fast reheating or the inflaton potential being locally ϕ^4 , as in Higgs inflation [25]. The scale factor $a(\eta)$ is chosen such that it describes a smooth transition from inflation at early times to radiation domination [11],

$$a(\eta) = \left\{ \left(\frac{1}{a_e H_e} - \eta \right)^{-1} H_e^{-1} \text{ for } \eta \leq 0 , \quad a_e^2 H_e \left(\eta + \frac{1}{a_e H_e} \right) \text{ for } \eta > 0 \right\} , \quad (31)$$

$$H(\eta) = \{ H_e \text{ for } \eta \leq 0 , \quad H_e (a_e/a)^2 \text{ for } \eta > 0 \} , \quad (32)$$

where a_e and H_e are the scale factor and the Hubble rate at the end of inflation, respectively; $H(\eta) = a'/a^2$ in terms of the conformal time. At $\eta \gg \frac{1}{a_e H_e}$, a simple scaling holds,

$$\eta \propto a ,$$

which simplifies the EOM. In our numerical analysis, we use the full $a(\eta)$ dependence as above.

The Higgs condensate and the fermion mass stay constant until the Hubble rate reduces to the level of the Higgs effective mass,

$$H \simeq \sqrt{3\lambda_h} \langle h \rangle . \quad (33)$$

At this stage, the condensate starts oscillating in a quartic potential and scaling down in a radiation-like manner. The oscillations produce gauge bosons and other SM states, leading to fast condensate decay, within $\mathcal{O}(10)$ oscillations [26]. We denote the corresponding scale factor by a_0 and parametrize the results in terms of

$$a_0/a_e \equiv N \sim \mathcal{O}(\text{few}) . \quad (34)$$

At this stage, the fermion mass starts changing fast, possibly dropping substantially. In our numerical analysis, we typically take $N = 6$ to account for both the Hubble rate reduction (33) and finite decay time of the condensate, although this only gives a ballpark estimate.

In what follows, we consider two possibilities for the $M(\eta)$ dependence. The simplest option is to use the step-function approximation, which corresponds to fast condensate decay and no other significant mass contributions. The second option is motivated by thermal effects, in which case the mass term decays more slowly, as a power law in a .

3.2.1 Step-function mass term

To account for a fast drop in the fermion mass, let us take the mass function of the form $M\theta(\eta_0 - \eta) + m\theta(\eta - \eta_0)$ with $M \gg m$. That is,

$$-\infty < \eta < \eta_0 : M(\eta) = M \quad (35)$$

$$\eta_0 < \eta < \infty : M(\eta) = m, \quad (36)$$

where η_0 corresponds to the scale factor a_0 in (34). For this mass function, the inflationary *in* solution retains the standard form, while the *out* solution must be recalculated. In what follows, we focus on the *out* wavefunction and drop the superscript *out* for convenience, while restoring it when necessary.

out wavefunction, $\eta > \eta_0$. At $\eta > \eta_0$, the EOM for u_A is

$$u_A'' + (k^2 + im a_e^2 H_e + \eta^2 m^2 a_e^4 H_e^2) u_A = 0, \quad (37)$$

while the EOM for u_B is obtained by replacing $m \rightarrow -m$. The boundary condition is

$$\begin{pmatrix} u_A \\ u_B \end{pmatrix} \xrightarrow{\eta \rightarrow \infty} \begin{pmatrix} 1 \\ \frac{k}{2am} \end{pmatrix} e^{-i \int \omega(\eta) d\eta}, \quad (38)$$

with $\omega \rightarrow a(\eta)m$. The solution is a parabolic cylinder function $D_\nu(z)$. Defining

$$C = \frac{k^2}{2ma_e^2 H_e}, \quad (39)$$

we find

$$u_A(\eta) = e^{-\frac{\pi}{4}C} D_{-iC} \left(e^{i\pi/4} \sqrt{\frac{2m}{H(\eta)}} \right) \times \text{phase}, \quad (40)$$

where the time-dependent phase is universal for u_A and u_B , and thus irrelevant for our purposes.³ The u_B part of the wavefunction is

$$u_B(\eta) = \sqrt{C} e^{-\frac{\pi}{4}C + \frac{i\pi}{4}} D_{-1-iC} \left(e^{i\pi/4} \sqrt{\frac{2m}{H(\eta)}} \right) \times \text{phase}, \quad (41)$$

where the “phase” is the same as that in u_A .

out wavefunction, $\eta \leq \eta_0$. The EOM is obtained from (40) by the replacement $m \rightarrow M$ with the addition of the delta-function term at η_0 . The delta function can be traded for a derivative jump in the boundary conditions, which can also be obtained directly from (15),

$$u'_A \Big|_- = u'_A \Big|_+ - ia_0(M - m) u_A(\eta_0), \quad (42)$$

where “-” and “+” refer to the limits from below and above η_0 , respectively. An analogous relation applies to u_B up to $m, M \rightarrow -m, M$. Although the solution can be expressed as a combination

³This phase is suppressed by $\ln \eta/\eta^2$ at large η .

of the parabolic cylinder functions, it is more physically meaningful to resort to approximations. Since $N \sim \mathcal{O}(\text{few})$, the η^2 term at $\eta < \eta_0$ is suppressed by

$$N^2 \frac{M}{H_e} \ll 1 \quad (43)$$

compared to the constant $MH_e a_e^2$ term and can be neglected.⁴ We thus obtain an equation with a constant frequency,

$$u_A'' + \alpha u_A = 0 \quad , \quad \alpha \simeq k^2 + iM a_e^2 H_e \quad , \quad (44)$$

which is solved by

$$u_A = a_1 e^{i\sqrt{\alpha}\eta} + a_2 e^{-i\sqrt{\alpha}\eta} \quad , \quad (45)$$

with constant a_i . Similarly,

$$u_B = b_1 e^{i\sqrt{\alpha^*}\eta} + b_2 e^{-i\sqrt{\alpha^*}\eta} \quad . \quad (46)$$

The boundary condition on $u_{A,B}$ and their derivatives at η_0 determines the coefficients a_i, b_i . The Bogolyubov coefficient can be evaluated at η_e , which, for our purposes, we may approximate by $\eta \sim 0$, hence we aim at computing

$$u_A(0) = a_1 + a_2 \quad , \quad u_B(0) = b_1 + b_2 \quad . \quad (47)$$

The wavefunction is continuous and its value at $\eta = \eta_0$ is determined by the small-mass solution. Since

$$H(\eta_0) \gg m \quad , \quad (48)$$

we can use the $z \rightarrow 0$ expansion

$$D_\nu(z) \simeq \frac{\sqrt{\pi} 2^{\nu/2}}{\Gamma(-\frac{\nu}{2} + \frac{1}{2})} - \frac{\sqrt{\pi} 2^{\nu/2+1/2}}{\Gamma(-\frac{\nu}{2})} z \quad , \quad (49)$$

together with

$$|\Gamma(it)| = \sqrt{\frac{\pi}{t \sinh \pi t}} \quad , \quad |\Gamma(it + 1/2)| = \sqrt{\frac{\pi}{\cosh \pi t}} \quad , \quad |\Gamma(it + 1)| = \sqrt{\frac{\pi t}{\sinh \pi t}} \quad , \quad (50)$$

valid for a real t . Up to an overall phase, we have the following expansion in the vicinity of η_0 ,

$$\begin{aligned} u_A(\eta \geq \eta_0) &\simeq e^{-\pi C/4} 2^{-iC/2} \sqrt{\pi} \left[\frac{1}{\Gamma(iC/2 + 1/2)} - \frac{\sqrt{2} e^{i\pi/4} \sqrt{2m a_e^2 H_e}}{\Gamma(iC/2)} \eta \right] \quad , \quad (51) \\ u_B(\eta \geq \eta_0) &\simeq \sqrt{C} e^{-\pi C/4 + i\pi/4} 2^{-iC/2 - 1/2} \sqrt{\pi} \left[\frac{1}{\Gamma(iC/2 + 1)} - \frac{\sqrt{2} e^{i\pi/4} \sqrt{2m a_e^2 H_e}}{\Gamma(iC/2 + 1/2)} \eta \right] \quad . \end{aligned}$$

These expressions fix the wavefunction value together with its derivative at η_0 .

As is clear from the expression for the frequency squared α , there are two distinct regimes for the wavefunction evolution at $\eta < \eta_0$. At

$$k^2 \ll M a_e^2 H_e \quad , \quad (52)$$

⁴This condition implies that the Hubble rate at the time of the condensate decay H_0 is far above the fermion mass M .

the evolution is different for u_A and u_B , while for large momenta it is universal. The non-universality is important for the Bogolyubov coefficient, which measures the degree of misalignment between the *in* and *out* vectors, hence it is only significant below the critical momentum value. In the regime $k^2 \ll Ma_e^2 H_e$, we obtain (up to a phase)

$$\begin{aligned} u_A(0) &\simeq e^{-\pi C/4} 2^{-iC/2} \sqrt{\cosh \frac{\pi C}{2}} \times \left(1 + i \frac{N^2}{2} \frac{M}{H_e} + \mathcal{O}\left(\frac{k}{a_e H_e}\right) \right) , \\ u_B(0) &\simeq e^{-\pi C/4} 2^{-iC/2} \sqrt{\sinh \frac{\pi C}{2}} \times \left(1 - i \frac{N^2}{2} \frac{M}{H_e} + \mathcal{O}\left(\frac{k}{a_e H_e}\right) \right) , \end{aligned} \quad (53)$$

where the universal $\mathcal{O}\left(\frac{k}{a_e H_e}\right)$ terms cancel in the Bogolyubov coefficient. The C -dependent prefactors correspond to $u_{A,B}$ based on mass m and the net result of the mass change at η_0 amounts to the rotation of u_A and u_B by opposite phases of order $N^2 \frac{M}{H_e}$.

At large k , the EOM and the derivative jump are dominated by the universal k^2 term, such that the non-universal phase is suppressed by M/k . The resulting Bogolyubov coefficient would also be suppressed.

***in* wavefunction.** During inflation, the mass term variation is determined by the relaxation time of the Higgs field, $(\sqrt{\lambda_h} H)^{-1}$, which gives a contribution to the EOM suppressed by $\sqrt{\lambda_h} \ll 1$. Hence, the mass term changes adiabatically and the EOM can be approximated by

$$\eta^2 u_A'' + \left(k^2 \eta^2 + \left[\frac{iM}{H_e} + \frac{M^2}{H_e^2} \right] \right) u_A = 0 , \quad (54)$$

where M is taken to be constant at the later stages of inflation and determined by the terminal value of the Higgs field $\langle h \rangle$. This is an adequate approximation for computing the Bogolyubov coefficient at $\eta \sim \eta_e$. The EOM for u_B is obtained by replacing $M \rightarrow -M$.

At $\eta \rightarrow -\infty$, the mass term plays no role and we have the usual Bunch-Davies boundary condition

$$\begin{pmatrix} u_A \\ u_B \end{pmatrix} \stackrel{\text{in}}{\underset{\eta \rightarrow -\infty}{\longrightarrow}} \begin{pmatrix} 1/\sqrt{2} \\ 1/\sqrt{2} \end{pmatrix} e^{-ik\eta} . \quad (55)$$

The solution is given by the Hankel functions,

$$u_A^{in}(a) = \sqrt{\frac{\pi k}{4aH_e}} e^{i\frac{\pi}{2}(1-iM/H_e)} H_{1/2-iM/H_e}^{(1)}\left(\frac{k}{aH_e}\right) , \quad (56)$$

$$u_B^{in}(a) = \sqrt{\frac{\pi k}{4aH_e}} e^{i\frac{\pi}{2}(1+iM/H_e)} H_{1/2+iM/H_e}^{(1)}\left(\frac{k}{aH_e}\right) . \quad (57)$$

We are interested in the momentum range $\frac{k}{a_e H_e} \ll 1$, which can potentially give significant occupation numbers. Hence, we may use the small argument expansion

$$H_\nu^{(1)}(x) \simeq -\frac{i2^\nu \Gamma(\nu)}{\pi} x^{-\nu} . \quad (58)$$

At the end of inflation ($a \simeq a_e$), we thus find

$$\begin{aligned} u_A &\simeq \frac{1}{\sqrt{2}} \times e^{i\frac{M}{H_e} \ln \frac{k}{a_e H_e}} , \\ u_B &\simeq \frac{1}{\sqrt{2}} \times e^{-i\frac{M}{H_e} \ln \frac{k}{a_e H_e}} , \end{aligned} \quad (59)$$

where we have neglected terms of order M/H_e not enhanced by any additional factors.

Particle number. The Bogolyubov coefficient $|\beta_k| = |u_{A,k}^{in}u_{B,k}^{out} - u_{B,k}^{in}u_{A,k}^{out}|$, can be evaluated at $\eta \sim \eta_e$, where our *in* and *out* solutions give a good approximation to the true wavefunctions. Using (53) and (59), we find that at $C \ll 1$, the *out* wavefunction is proportional to $(1, 0)^T$, while the *in* wavefunction has the form $(1/\sqrt{2}, 1/\sqrt{2})^T$ up to small corrections. Hence, the Bogolyubov coefficient is close to $1/\sqrt{2}$. For larger momenta, $C > 1$, but still below $\sqrt{Ma_e^2 H_e}$, both *in* and *out* wavefunctions are close to $(1/\sqrt{2}, 1/\sqrt{2})^T$, yet the cancellation in the Bogolyubov coefficient is incomplete and the leading order result is

$$|\beta_k| \simeq \frac{1}{2} \frac{M}{H_e} \left| N^2 - 2 \ln \frac{k}{a_e H_e} \right|. \quad (60)$$

For $N \sim 6$, the $\ln k$ term can be neglected and $|\beta_k|$ is approximately constant in this momentum window. At yet larger $k \gtrsim \sqrt{Ma_e^2 H_e}$, the constant term disappears and $|\beta_k|$ drops further, approaching zero at very large momenta.

Our results are summarized as:

$$\begin{aligned} k \ll k_* &: |\beta_k| \simeq \frac{1}{\sqrt{2}}, \\ k_* \lesssim k \ll \tilde{k}_* &: |\beta_k| \simeq \frac{1}{2} N^2 \frac{M}{H_e}, \\ \tilde{k}_* \lesssim k &: |\beta_k| \simeq 0, \end{aligned} \quad (61)$$

with

$$k_* = \sqrt{2ma_e^2 H_e}, \quad \tilde{k}_* = \sqrt{2Ma_e^2 H_e}, \quad (62)$$

where we have defined \tilde{k}_* with a factor of $\sqrt{2}$ for uniformity of notation. Fig. 2 shows representative results of our numerical analysis, which does not resort to the approximations made above. One clearly sees the step-like features in $|\beta_k|^2$ with the appropriate momentum cutoffs, as expected from our analytical estimates.

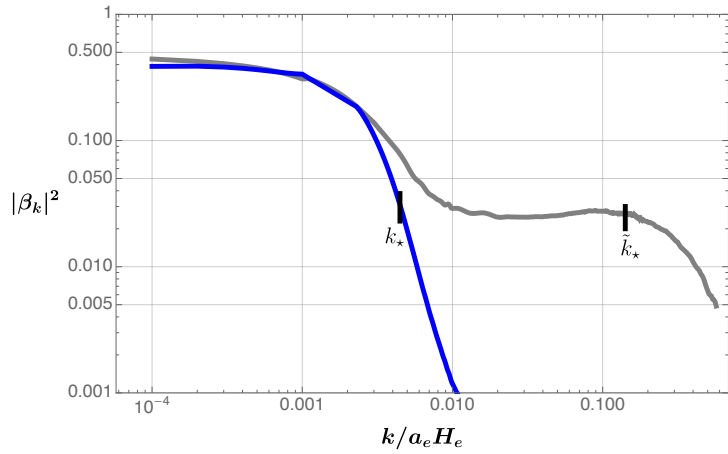


Figure 2: Bogolyubov coefficient squared for a constant fermion mass (blue) and piece-wise constant mass (grey). Radiation domination after inflation is assumed and $m = 10^{-5} H_e$, $M = 10^{-2} H_e$, $N = 6$.

The particle number depends on the momentum cutoff cubed. Thus, for a large hierarchy between m and M , the main contribution to the particle density comes from the momentum range between k_* and \tilde{k}_* , even though the corresponding average occupation number is small. In this case, we may approximate the particle density produced via inflation by

$$n \sim 4 \times \int \frac{d^3\mathbf{k}}{(2\pi)^3 a^3} \theta(\tilde{k}_* - k) |\beta_k|^2, \quad (63)$$

where $|\beta_k|$ corresponds to the momentum range $k_* < k < \tilde{k}_*$ and the factor of 4 comes from the spin d.o.f. of a Dirac field. Thus,

$$n \sim \frac{2}{3\pi^2} \tilde{k}_*^3 \frac{1}{a^3} |\beta_k|^2 = \frac{\sqrt{2}}{3\pi^2} N^4 \frac{M^{7/2}}{H_e^{1/2}} \frac{a_e^3}{a^3}. \quad (64)$$

This result is dominated by the high momentum modes up to \tilde{k}_* , which have a low average occupation number of order $N^4 M^2 / H_e^2$. Note that this quantity can be expressed as M^2 / H_0^2 , where H_0 is the Hubble rate at the time of the condensate decay.

The particle abundance is computed according to

$$Y = \frac{n}{s_{\text{SM}}} , \quad s_{\text{SM}} = \frac{2\pi^2 g_*}{45} T^3 , \quad (65)$$

where s_{SM} is the entropy density of the SM thermal bath with temperature T and g_* is the effective number of degrees of freedom in the SM bath. This is a meaningful quantity if the particle number is conserved after the production process has completed. In our case, particle production is independent of m and occurs at the early postinflationary stage, not far from the condensate decay time, hence Y is conserved after that. The result is independent of the reheating temperature as long as the Universe is radiation-like, which could be due to the inflaton oscillations in the ϕ^4 potential. We find

$$Y \sim 10^{-3} \times N^4 \frac{M^{7/2}}{M_{\text{Pl}}^{3/2} H_e^2}. \quad (66)$$

This gives the abundance of gravitationally produced particles in the regime $m \ll M \ll H_e$ in the case of a short-lived condensate, $N^2 M / H_e \ll 1$, which decays abruptly. Here $N \geq 1$ controls the lifetime of the scalar condensate and for the Higgs field one expects $N \sim \mathcal{O}(\text{few})$.

In the case of the Higgs-induced masses, one may rewrite this result in a more palatable form. For instantaneous condensate decay at $a = a_0$, we have $H_e / N^2 = H_0 \sim \sqrt{3\lambda_h} \langle h \rangle \simeq \sqrt{3\lambda_h} H_e$. Since $M \sim Y_f H_e$, the fermion abundance can be estimated by

$$Y^{\text{SM}} \sim 10^{-3} \times \frac{Y_f^{7/2}}{\lambda_h} \left(\frac{H_e}{M_{\text{Pl}}} \right)^{3/2}, \quad (67)$$

up to the color multiplicity factor. For large H_e , this result is enhanced by many orders of magnitude compared to the naive estimate based on the electroweak fermion masses, $Y^{\text{SM}} \sim 10^{-26} Y_f^{3/2}$. In particular, with $H_e \sim 10^{13} \text{ GeV}$, our result is larger by a factor of $10^{19} Y_f^2$.

One should keep in mind that our considerations apply to fermion production due to the time-dependent background. There are, of course, other, more powerful, sources of the SM fermions such as the direct inflaton decay, etc. These create the thermal bath that enters into the Y

calculation. While for the SM fermions our analysis does not affect the conventional approach to reheating⁵, inflationary particle production can be the leading source for very weakly interacting fermions such as the right-handed neutrinos.

3.2.2 Slow effective mass decrease and thermal effects

The transition from a large mass M to a small mass m in reality is expected to be smooth rather than abrupt. This can be due to generation of the effective fermion mass by “medium” effects, for example, via interaction with the thermal bath. The thermal mass may be very large soon after inflation but vanish at late times.

In what follows, we *model* the transition to the small mass regime using thermal effects as a template. Instead of performing the thermal QFT analysis in curved space, we parametrize the time dependence of the effective fermion mass in accordance with the thermal QFT expectations. This should capture the main features of fermion production in a more realistic setting.

We treat the thermal bath as the “medium” which creates an effective mass due to the coupling to the gauge bosons, but *does not directly produce fermions* itself. In this approach, particle production occurs due to the background and mass time dependence in the Dirac equation, which differs from the direct particle production via, for example, the inflaton decay. Strictly speaking, of course, the gauge and gravitational effects are entangled in this system. Yet, our analysis is helpful and our core results apply more generally, beyond the thermal mass approximation.

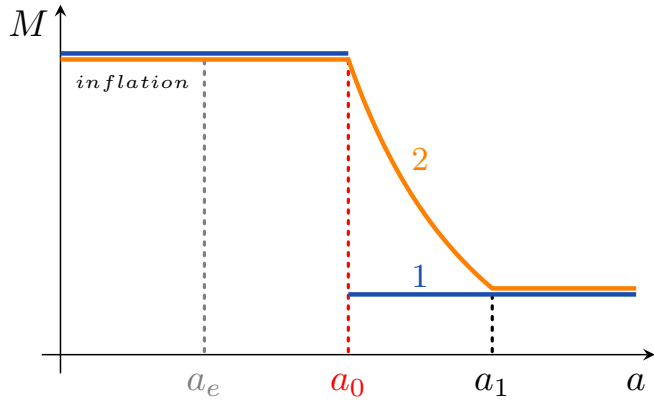


Figure 3: Effective fermion mass evolution: (1) abrupt, (2) smoothed by thermal effects.

In what follows, we compute the Bogolyubov coefficient based on a continuous $M(a)$ function with

$$M \propto T \propto 1/a ,$$

as long as the thermal mass dominates. Here T is the SM bath temperature and the above scaling assumes fast reheating, i.e. the SM thermal bath takes over the energy balance around the condensate decay time or even earlier. We model the $M(\eta)$ function with 3 distinct periods (Fig. 3):

⁵Inflationary SM fermion production can be relevant to models where the inflaton decays exclusively to the hidden sector states.

- (1) $\eta < \eta_0$: large constant mass M
- (2) $\eta_0 < \eta < \eta_1$: thermal mass $M(\eta) \propto 1/a$
- (3) $\eta_1 < \eta$: small constant mass m

The next step is to compute the *out* solution by solving the EOM in each period and matching them at the boundaries. The *in* solution remains the same as before, hence we focus entirely on the *out* wavefunction and drop the *out* superscript. Since the $\eta \rightarrow \infty$ behavior remains unchanged, it is easiest to start with the late time period.

Late times. In the regime $\eta > \eta_1$, the solutions (40) and (41) apply. At late times, $H(\eta) \sim T^2/M_{\text{Pl}} \ll m$, hence one can use the large argument expansion of the parabolic cylinder function,

$$D_\nu(z) \simeq e^{-z^2/4} z^\nu ,$$

for $z \gg 1$, yielding

$$\begin{aligned} u_A(\eta) &\simeq e^{-i\frac{m}{2H(\eta)}} , \\ u_B(\eta) &\simeq \frac{k}{2m a(\eta)} e^{-i\frac{m}{2H(\eta)}} , \end{aligned} \quad (68)$$

neglecting the sub-leading phase contributions in the limit $m \gg H(\eta)$.⁶ In terms of the conformal time, the Hubble rate is given by $H = \frac{1}{a_e^2 H_e \eta^2}$.

This constant mass regime extends to the earlier times to the point where the thermal mass contribution becomes comparable to the bare mass,

$$m \sim gT , \quad (69)$$

where g denotes a generic gauge coupling responsible for the thermal mass. In the Standard Model, the Higgs-induced mass also changes due to the temperature dependence of the Higgs potential. In our context, however, this effect is unimportant.

Intermediate regime. For $\eta < \eta_1$, the thermal mass becomes more important than the bare mass. Since $T \propto 1/a$ in the SM radiation dominated Universe,

$$a M(a) \simeq \text{const} . \quad (70)$$

This applies to the period between a_0 and a_1 , hence $a_0 M \simeq a_1 m$. The EOM (24) take the form

$$u_A'' + (a^2 M(a)^2 + k^2) u_A = 0 \quad (71)$$

$$u_B'' + (a^2 M(a)^2 + k^2) u_B = 0 . \quad (72)$$

The equations are identical for u_A and u_B , and contain a constant frequency

$$\omega = \sqrt{a^2 M^2 + k^2} .$$

The solutions are

$$\begin{aligned} u_A &= a_1 e^{i\omega\eta} + a_2 e^{-i\omega\eta} , \\ u_B &= b_1 e^{i\omega\eta} + b_2 e^{-i\omega\eta} , \end{aligned} \quad (73)$$

⁶Note also that the positive energy asymptotic *out* states are obtained as an expansion in $k/(a m)$.

with constant a_i, b_i .

Consider the regime

$$k \ll a_1 m , \quad (74)$$

Let us first evaluate u_B . Matching the wavefunction value and its derivative at η_1 , one finds $b_1/b_2 = \mathcal{O}(k^2/(a_1^2 m^2))$ and

$$u_B(\eta < \eta_1) \simeq \frac{k}{2a_1 m} e^{-i\omega\eta} \times \text{const phase} . \quad (75)$$

Similarly,

$$u_A(\eta < \eta_1) \simeq e^{-i\omega\eta} \times \text{const phase} . \quad (76)$$

Therefore, at η_0 the wavefunction takes the form

$$\begin{pmatrix} u_A \\ u_B \end{pmatrix}(\eta_0) \sim \begin{pmatrix} 1 \\ 0 \end{pmatrix} \times \text{phase} , \quad (77)$$

up to corrections of order $\frac{k}{a_1 m}$. Thus, it retains its $\eta \rightarrow +\infty$ asymptotic form. This is a feature of the constant frequency evolution in the period $\eta_0 < \eta < \eta_1$.

As k approaches $a_1 m$, the wavefunction initial condition at η_1 tends to the democratic form close to $(1/\sqrt{2}, 1/\sqrt{2})^T$. This form is retained by the constant frequency evolution from η_1 to η_0 . Thus $k \sim a_1 m = a_0 M$ represents the momentum cutoff for our considerations and, for larger momenta, there are significant cancellations in the Bogolyubov coefficient.

Early times. The evolution from η_0 to η_e proceeds as before. It amounts to a small rotation of the wavefunction by a phase of order $N^2 M/H_e$. This is a subleading effect in the present case and we may neglect it.

Particle number. The *in* wavefunction remains of the form $(1/\sqrt{2}, 1/\sqrt{2})^T$ for the entire momentum range of interest. The *out* wavefunction has the form $(1, 0)^T$ for the momenta below $a_0 M$, hence we may approximate

$$\begin{aligned} k \lesssim k_*^{\text{th}} &: |\beta_k| \simeq 1/\sqrt{2} , \\ k > k_*^{\text{th}} &: |\beta_k| \simeq 0 , \end{aligned} \quad (78)$$

where the ‘‘thermal’’ cutoff is

$$k_*^{\text{th}} = a_0 M . \quad (79)$$

Our numerical results are shown in Fig. 4, left panel. They exhibit good agreement with the analytical estimates, in particular, in terms of the position of the momentum cut-off.

Using the $\theta(k_*^{\text{th}} - k)$ approximation in the Bogolyubov coefficient, we find

$$n \sim \frac{1}{3\pi^2} N^3 M^3 \frac{a_e^3}{a^3} , \quad (80)$$

and

$$Y \sim 10^{-3} \times N^3 \frac{M^3}{(M_{\text{Pl}} H_e)^{3/2}} . \quad (81)$$

This is larger than our previous result by the factor $(N\sqrt{M/H_e})^{-1}$, so we conclude that

$$Y_{\text{fast}} \sim Y_{\text{slow}} \times N \sqrt{\frac{M}{H_e}} \ll Y_{\text{slow}} ,$$

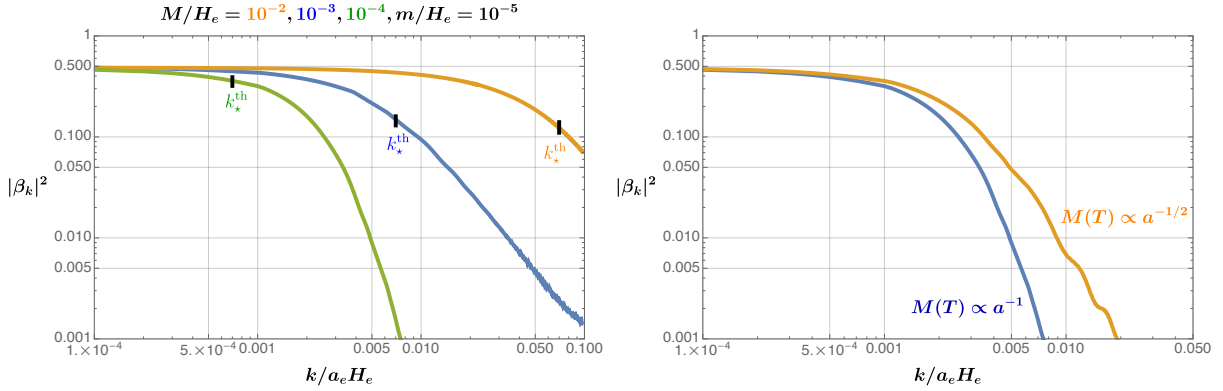


Figure 4: Bogolyubov coefficient squared for a fermion with a thermal mass during radiation domination. *Left:* The orange, blue, green curves correspond to $M/H_e = 10^{-2}, 10^{-3}, 10^{-4}$, respectively, and $m/H_e = 10^{-5}$. The occupation number drops above k_*^{th} . *Right:* Comparison of the results for different thermal mass scaling laws: $M(T) \propto a^{-1}$ vs $M(T) \propto a^{-1/2}$, with the other parameters fixed.

where the subscripts “slow” and “fast” refer to the slow and fast fermion mass variation after the scalar condensate decay.

So far we have worked in the approximation that the thermal mass is similar to the Higgs-induced mass. However, our results apply more generally. Let us consider some variations of our assumptions.

- *different mass scaling.* If the SM thermal bath is subdominant in the energy balance, its energy density scales as $1/a^2$ and the corresponding temperature scales as $1/a^{1/2}$ (see, e.g. [27]). This changes the fermion mass scaling to $M(a) \propto a^{-1/2}$. We find that the resulting effect on the Bogolyubov coefficient is insignificant, in particular, the momentum cutoff remains almost the same (Fig. 4, right panel).
- *sharp features in $M(\eta)$.* At early times $\eta \sim \mathcal{O}(\eta_0)$, the effective fermion mass can change abruptly due to fast non-perturbative effects. Also, the thermal mass could grow larger than that induced by the Higgs condensate. To understand the influence of such effects, consider an abrupt fermion mass change:

$$M(\eta) = M \theta(\eta_0 - \eta) + \mathcal{M} \theta(\eta - \eta_0) \quad , \quad M \ll \mathcal{M} \ll H_e .$$

The wavefunction analysis is completely analogous to our earlier calculations with the result

$$u_A(0) = u_A(\eta_0) \left[1 + \mathcal{O}\left(\frac{\mathcal{M}}{H_e} N^2\right) \right] ,$$

omitting the irrelevant terms for computing the Bogolyubov coefficient. Therefore, the correction is small as long as the largest mass is significantly below the Hubble rate, $N \sqrt{\mathcal{M}/H_e} \ll 1$. The Bogolyubov coefficient is determined primarily by the “thermal” mass, which decreases slowly over a long period, rather than abrupt mass variations at $\eta \lesssim \eta_0$. This is also confirmed by our numerical analysis.

Our conclusion is that the above result is quite stable to variations of the thermal mass scaling and introduction of sharp features into the mass function. Note also a significant degree

of flavor universality of the result: although the scale $a_1(m_f)$ is flavor dependent and defined by $g T(a_1) \sim m_f$, the combination $a_1(m_f) m_f = a_0 M$ is flavor independent and it is this product that determines the abundance.

4 Standard Model fermion and right-handed neutrino production via inflation

In this section, we discuss inflationary production of the SM fermions as well as right-handed neutrinos. Classical gravity is responsible for production of the SM states irrespectively of the inflaton couplings, which is an omnipresent effect in standard cosmology. For the right-handed neutrinos ν_R , this production channel can be particularly important given that their couplings could be very small. Since ν_R or, more generally, singlet fermions, may constitute dark matter, the question of inflationary particle production becomes all the more pressing. In what follows, we assume that inflation is followed by the radiation domination era, while the matter domination option will be discussed in Section 5.

4.1 Quark and lepton production

Our results apply directly to quark and lepton production via inflation. The Higgs condensate creates a large effective fermion mass which facilitates gravitational particle production. Its efficiency is sensitive to the post-inflationary wavefunction evolution. As is clear from the above discussion, one distinguishes two possibilities: in the first case, the effective mass drops abruptly to some small value, whereas in the second case, such a decrease happens over a long period, which we model by the thermal mass contribution. While the postinflationary dynamics remain largely unknown, a realistic situation is likely to fall in between these special cases.

4.1.1 Sharp effective mass decrease

This possibility corresponds to fast Higgs condensate decay, in the absence of other significant sources for the effective fermion mass. This is the case when the thermal or non-equilibrium effects on the fermion propagation can be neglected.

The production efficiency is flavor-dependent and controlled by the fermion Yukawa coupling Y_f . Since $M_f = \frac{1}{\sqrt{2}} Y_f \langle h \rangle$, for $\langle h \rangle \simeq H_e$ and a step-function mass profile, we get

$$n_f^{\text{fast}} \sim \mathcal{O}(10) \times N_c Y_f^{7/2} H_e^3 \frac{a_e^3}{a^3}, \quad (82)$$

where we have taken $N = 6$ and N_c is the color multiplicity. The resulting abundance (66) of heavier fermions is much larger than that for lighter fermions, as long as $M_f \ll H_e$. The production is most efficient at early times, not far from the Higgs condensate decay time.

It is instructive to compare this result to the particle density $n_f(m_f)$ computed with constant low energy fermion masses $m_f = \frac{1}{\sqrt{2}} Y_f v$. The ratio of the two is

$$\frac{n_f^{\text{fast}}}{n_f(m_f)} \sim \left(\frac{M_f}{m_f} \right)^{3/2} \times N^4 \frac{M_f^2}{H_e^2} \sim 10^{19} Y_f^2, \quad (83)$$

for $H_e \sim 10^{13}$ GeV. We observe that our result exceeds $n_f(m_f)$ by many orders of magnitude, e.g. 15 in the case of the bottom quark. For very light fermions, the discrepancy becomes smaller

due to the suppression factor Y_f^2 , which accounts for small average occupation numbers in the regime $N\sqrt{M_f/H_e} \ll 1$.

The energy density of the produced particles is dominated by the bottom quarks and remains tiny compared to that of the inflaton, $\rho_\phi \sim H^2 M_{\text{Pl}}^2$. Indeed, one can estimate or, more precisely, bound the characteristic energy of the fermion quantum by \tilde{k}_*/a_0 , which yields

$$\rho_f \lesssim Y_f^4 H_e^4 \sim M_f^4 \quad (84)$$

around the time of the condensate decay. Clearly, this contribution is unimportant for reheating, but can be significant in other contexts.

4.1.2 Slow effective mass decrease

This, presumably more realistic, option corresponds to the presence of significant thermal or non-equilibrium contributions to the fermion mass after the condensate has decayed. We model the effective mass decrease by the time-dependent thermal mass, although the results apply more generally. Of course, in order to create the thermal bath, there must be another mechanism for the SM particle production. Here, we only consider particle production via the *background evolution* in the Dirac equation and thus separate this mechanism from other sources.

Our analysis shows that the main factor in determining the particle production efficiency is the maximal thermal mass, whether it is above or below the condensate-induced effective mass. The result is given by (80) with M being the maximal thermal mass after the Higgs condensate decay. For fermions charged under $SU(N)$ and having the Yukawa couplings, the thermal mass is $M_f^2(T) = g^2 T^2 \frac{N^2-1}{16N} + |Y_f|^2 T^2 \frac{N_f}{16}$, where N_f is the particle multiplicity in the loop. Denoting the maximal temperature of the SM thermal bath by T_{max} , we find

$$n_f^{\text{slow}} \sim \alpha^3 g^3 N_c T_{\text{max}}^3 \frac{a_e^3}{a^3}, \quad (85)$$

where we have taken $N = 6$ and $M_f(T) = \alpha \times gT/\sqrt{6}$ as the benchmark value for a generic gauge coupling g , with $\alpha \sim \mathcal{O}(1)$ accounting for the different quantum numbers of the SM fermions. We observe that this result exhibits a significant degree of universality and the particle density generated via the Universe expansion on a thermal background can be significantly higher than that in (82). This is the case, for example, when the inflaton decays sufficiently fast generating a large maximal SM temperature [28],

$$T_{\text{max}} \sim (\Gamma_\phi H_e M_{\text{Pl}}^2)^{1/4},$$

with Γ_ϕ being the inflaton decay width. As in the previous case, the result is essentially independent of the low-energy fermion masses and dictated primarily by the early time particle production, when the temperature is not too far from T_{max} . We also find that the exact scaling of the temperature with time is not important, i.e. the results for $T \propto a^{-1}$ and $T \propto a^{-1/2}$ are similar.

The energy density of the produced particles is bounded by $n_f \times k_*^{\text{th}}/a_0$ at the time of the condensate decay, which again yields

$$\rho_f \lesssim M_f^4.$$

For $\Gamma_\phi \ll H_e$, this is far below the inflaton energy density, so our approximation is self-consistent. Unlike in the previous case, fermion production is almost democratic and determined primarily by the gauge couplings. Since there is no Yukawa coupling suppression, both the number and energy densities can by far exceed those corresponding to the sharp mass decrease case.

4.1.3 Top-quark production

In the case of the top-quark, the induced fermion mass is close to the Hubble rate and the approximation $M \ll H_e$ breaks down. The main effect of the mass increase is the change in the inflationary *in*-wavefunctions. As seen from (56,57), for $M \gtrsim H_e$, the *in*-vector rotates towards $(1, 0)^T$ since at the end of inflation

$$|u_A^{in}/u_B^{in}| \sim e^{\pi M/H_e} \gg 1 ,$$

which makes it proportional to the corresponding *out*-vector. Hence, even at small momenta, there is a significant cancellation in the Bogolyubov coefficient leading to a smaller average occupation number. The effect is *exponentially* sensitive to the fermion mass.

For the realistic value of the top Yukawa coupling, such suppression is not too strong and partially compensated by the increase in the momentum cutoff compared to that of lighter fermions. The result is exponentially sensitive to the precise value of the induced top quark mass, which depends on the poorly constrained $\lambda_h(H_e)$. We choose the benchmark values $M_t = 0.4H_e$ and $0.7H_e$, for which we find, assuming the step-function mass term,

$$\begin{aligned} M_t = 0.4H_e : \quad & |\beta_k|^2 \simeq 0.4 , \quad k_* \simeq 10^{-4} a_e H_e , \\ M_t = 0.7H_e : \quad & |\beta_k|^2 \simeq 0.3 , \quad k_* \simeq 10^{-3} a_e H_e . \end{aligned} \quad (86)$$

With the smoothed time variation of the effective top-quark mass as motivated by the thermal effects ($M \propto 1/a$), we obtain

$$\begin{aligned} M_t = 0.4H_e : \quad & |\beta_k|^2 \simeq 0.07 , \quad k_*^{\text{th}} \simeq 0.2 a_e H_e , \\ M_t = 0.7H_e : \quad & |\beta_k|^2 \simeq 0.01 , \quad k_*^{\text{th}} \simeq 0.6 a_e H_e . \end{aligned} \quad (87)$$

Both the Bogolyubov coefficient and the momentum cutoff change compared to those of lighter fermions. This is expected since $N\sqrt{M_t/H_e} \gg 1$ and it cannot be used as an expansion parameter.

The resulting top-quark number density with the step-function $M(\eta)$ dependence is

$$n_t^{\text{fast}} \sim 10^{-11} \times N_c H_e^3 \frac{a_e^3}{a^3} , \quad (88)$$

assuming $M_t = 0.7H_e$ and N_c is the color multiplicity. Therefore, the top-quark production in this approximation is *suppressed* compared to that of intermediate mass fermions b, c, τ , but is still more efficient than production of light fermions like u, d, e .

For a thermal-like mass profile, the density is much larger,

$$n_t^{\text{slow}} \sim 10^{-4} \times N_c H_e^3 \frac{a_e^3}{a^3} , \quad (89)$$

with $M_t = 0.7H_e$. This mass value corresponds to a large maximal temperature, around the Hubble scale. At such a high temperature, all the SM fermion thermal masses are of the same order of magnitude, so the top-quark is not special and the particle abundance is flavor-universal. This result shows some suppression of the fermion production when the thermal mass becomes comparable to H_e (cf. Eq. 85).

4.1.4 No Higgs condensate

The main assumption of our work is that a large Higgs condensate forms in the Early Universe. This is not necessarily the case. In the presence of a large effective mass during inflation, the Higgs field rolls to the potential minimum. This happens if there is a tangible Higgs-inflaton coupling $\lambda_{\phi h} \varphi^2 h^2$ or a non-minimal Higgs coupling to gravity $\xi h^2 R$, with the appropriate sign as to generate a positive effective mass term [29]. In case such a mass term is around or above the Hubble rate, the Higgs dynamics are essentially classical and the field is confined to the origin.

Formation of the Higgs condensate is essential for particle production in the case of the step-function profile of $M(\eta)$. Thus, $\langle h \rangle \ll H_e$ would eliminate this production mechanism. On the other hand, if the fermion attains a large thermal mass soon after the end of inflation, its production becomes significant. The inflationary *in*-wavefunction at $\eta \sim 0$ remains close to $(1/\sqrt{2}, 1/\sqrt{2})^T$, such that the results of Sec. 3.2.2 largely apply and the particle number density has the form (85).

We note that the existence of the thermal mass does not necessarily imply that the particle itself is part of the thermal bath [30]. Indeed, a non-thermal ν_R can have a substantial thermal mass due to its Yukawa coupling, which represents ‘‘friction’’ for the neutrinos propagating in a medium. In this case, inflationary particle production via the background evolution can be clearly separated from other sources.

Let us summarize our findings so far. Inflationary fermion production is sensitive to the Early Universe dynamics such that no precise prediction can be made. In particular, the production efficiency depends on the postinflationary wavefunction. The latter is affected by the time-dependent profile of the effective mass function, which includes thermal/non-equilibrium effects in addition to the Higgs condensate evolution. In all the cases, however, the energy transfer to the quarks and leptons is very small compared to the inflaton energy.

4.2 Inflationary production of the right-handed neutrinos due to the Higgs coupling

Let us now apply our results to production of the right-handed neutrinos. In what follows, we assume that the ν_R couplings are small enough such that they do not thermalize and that ν_R are not produced directly via inflaton decay. In this case, there are 3 main sources of neutrinos: gravitational production due to the background evolution, decay of the Higgs condensate and the freeze-in mechanism. Here we focus on the effects of the Higgs Yukawa coupling \mathcal{Y}_ν , while the Majorana mass effects will be considered in the next subsection.

4.2.1 Production of ν_R due to the background evolution

In the Early Universe, the right-handed neutrinos attain a tangible mass via their Higgs couplings \mathcal{Y}_ν . This can be either due to the formation of the inflationary Higgs condensate or due to the thermal mass of order $\mathcal{Y}_\nu T$, which affects neutrino propagation in the thermal background. In the latter case, the result (81) applies with $M \sim \mathcal{Y}_\nu T/\sqrt{8}$ such that

$$Y_{\nu_R}^{\text{grav}} \sim 10^{-2} \mathcal{Y}_\nu^3 \frac{T_{\text{max}}^3}{(M_{\text{Pl}} H_e)^{3/2}}, \quad (90)$$

with $N = 6$. We note that this equation does not assume thermalization of the right-handed neutrinos⁷ and also applies to a non-thermal environment where the effective mass is created by non-equilibrium effects which fade away sufficiently slowly.

In the case of the step-function evolution of the neutrino mass, the abundance involves a higher power of \mathcal{Y}_ν and is typically smaller than the above estimate (cf. Eq. 66).

4.2.2 Direct neutrino production from the primordial Higgs condensate

The Higgs condensate formed at the inflationary stage decays into the SM states, which provides an additional source of quarks, leptons and right-handed neutrinos. Let us estimate the corresponding ν_R abundance.

After the condensate starts oscillating in the $\lambda_h h^4$ potential at $a \sim a_0$, it can be treated as “radiation”. The energy density of the neutrinos ρ_ν is obtained by solving the evolution equations

$$\dot{\rho}_h + 4H\rho_h = -\Gamma_h \rho_h , \quad (91)$$

$$\dot{\rho}_\nu + 4H\rho_\nu = \Gamma_{h_\nu} \rho_h , \quad (92)$$

where ρ_h is the Higgs condensate energy density, Γ_h is its decay width, Γ_{h_ν} is the Higgs condensate decay width into neutrinos, and the factor of 4 indicates the radiation-like scaling of the condensate and ν energy density. The solution is

$$a^4 \rho_\nu = \frac{\Gamma_{h_\nu}}{\Gamma_h} (1 - e^{-\Gamma_h t}) (a^4 \rho_h)_0 , \quad (93)$$

where ρ_{h0} is the initial energy density of the condensate at a_0 . The decay happens quite quickly, within an $\mathcal{O}(10)$ -fold increase of the scale factor [26]. The neutrino share of the initial condensate energy is controlled by the branching ratio

$$\frac{\Gamma_{h_\nu}}{\Gamma_h} \sim \mathcal{Y}_\nu^2 ,$$

which gives the right ballpark estimate for our purposes. Note that the decay $h \rightarrow \nu_L \nu_R$ is efficient only for

$$\mathcal{Y}_\nu \lesssim \sqrt{\lambda_h} ,$$

i.e. when the neutrinos are lighter than the Higgs.⁸

The initial Higgs condensate energy density is given by the Starobinsky-Yokoyama result [14],

$$\rho_{h0} \sim \frac{3H_e^4}{4\pi^2} , \quad (94)$$

and scales as a^{-4} after the condensate starts oscillating. The number density of the produced neutrinos can be estimated by taking the average energy of the produced quanta to be given by the effective Higgs mass (see e.g., [31, 12]),

$$E_{\nu_R} \sim m_h^{\text{eff}} = \sqrt{3\lambda_h} \langle h \rangle ,$$

⁷The ν_R thermal mass is created by the thermal particles in the loop, that is, the SM leptons and the Higgs field.

⁸For heavier neutrinos, the decay is exponentially suppressed and proceeds via the higher harmonics of the oscillating Higgs field.

with the Higgs condensate initial value H_e and $\langle h \rangle \propto 1/a$ for $a > a_0$. At the time of the condensate decay $a = a_d$ ⁹, we get

$$n_\nu(a_d) \sim \left(\frac{a_0}{a_d}\right)^3 \frac{\Gamma_{h\nu}}{\Gamma_h} H_e^3, \quad (95)$$

for $\lambda_h \sim 10^{-2}$. After that, the total number of ν_R is conserved, if we neglect other sources of ν_R -production.

The ν_R abundance is given by $Y_{\nu_R} = \frac{n_{\nu_R}}{s_{\text{SM}}}$, which remains constant after the Higgs condensate has decayed and reheating has completed. The scaling of the numerator and the denominator with a is the same, hence Y_{ν_R} can be computed at any convenient point, e.g. $a = a_d$. The result is

$$Y_{\nu_R}^{\text{higgs}} \sim 10^{-1} N^3 \mathcal{Y}_\nu^2 \left(\frac{H_e}{M_{\text{Pl}}}\right)^{3/2}, \quad (96)$$

where the superscript refers to the direct ν_R production from Higgs decay. As long as $T_{\text{max}} \lesssim H_e$, this is much larger than the neutrino abundance produced gravitationally $Y_{\nu_R}^{\text{grav}}$, with the inclusion of the thermal-like mass. The latter is suppressed by an additional power of \mathcal{Y}_ν and

$$\frac{Y_{\nu_R}^{\text{grav}}}{Y_{\nu_R}^{\text{higgs}}} < \mathcal{Y}_\nu \ll 1.$$

Hence, in this framework, gravitational fermion production gives only a subleading result.

4.2.3 Freeze-in ν_R production

Both contributions are dwarfed by the usual freeze-in production [32], in which case the abundance scales as [33]

$$Y_{\nu_R}^{\text{FI}} \sim \mathcal{Y}_\nu^2 \frac{M_{\text{Pl}}}{m_h}, \quad (97)$$

for $m_h \gg M_{\nu_R}$, where M_{ν_R} is the low energy neutrino mass scale. The production mode is $h \rightarrow \nu_L \nu_R$, which becomes most efficient at $T \sim m_h$. For $m_h \lesssim M_{\nu_R}$, the neutrino production proceeds via $hh \rightarrow \nu_R \nu_R$, which is most efficient at $T \sim M_{\nu_R}$ such that the scaling (97) holds up to the replacement $m_h \rightarrow M_{\nu_R}$.

For a very heavy ν_R , $M_{\nu_R} \gg m_h$, the freeze-in production involves a higher power of \mathcal{Y}_ν and it could also be Boltzmann-suppressed [34]. In this case, the Higgs condensate decay can be a competitive neutrino source.

Our conclusion is that gravitational ν_R production is superseded by that from the Higgs condensate decay. The latter, in turn, is swamped by the standard freeze-in production, unless the right-handed neutrinos are very heavy. Therefore, we find the following hierarchy,

$$Y_{\nu_R}^{\text{grav}} \ll Y_{\nu_R}^{\text{higgs}} \ll Y_{\nu_R}^{\text{FI}}.$$

4.3 Inflationary right-handed neutrino production due to the singlet scalar coupling

The inflationary right-handed neutrino production due to the Higgs Yukawa couplings cannot be the leading source of ν_R in typical cosmological settings. However, this conclusion does not

⁹In our previous fermion production analysis, we have loosely associated a_0 with the condensate oscillation and decay, whereas here we separate a_0 and a_d .

apply to the ν_R coupling to a singlet scalar s . Unlike the Higgs field, the new scalar can have a very small self-coupling, which suppresses the ν_R production from the condensate decay and also precludes thermalization. In this case, gravitational production can be the leading source of the right-handed neutrinos.

The scalar condensate can be long-lived, $N \gg 1$, which invalidates our expansion in $N \sqrt{M/H_e}$. Let us consider the large N case more closely, assuming a non-thermal system and a step-function fermion mass variation.

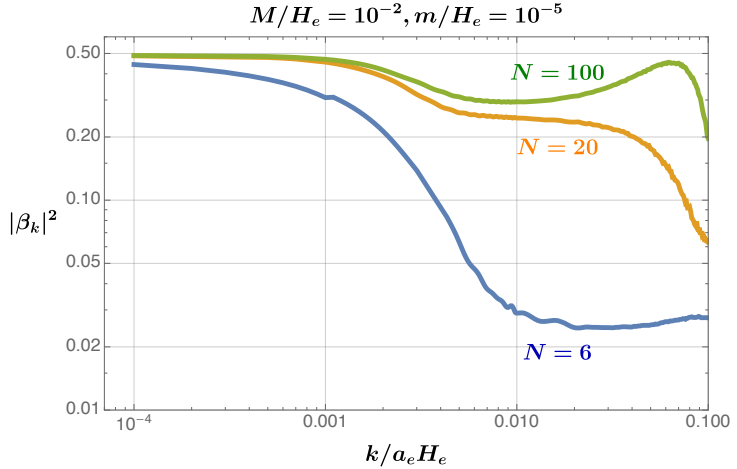


Figure 5: Bogolyubov coefficient squared for $N = 6, 20, 100$ and step-function mass variation. Radiation domination after inflation is assumed and $m = 10^{-5}H_e$, $M = 10^{-2}H_e$. At large N , the curves approach the single mass $|\beta_k|^2$ with the momentum cutoff $M^{1/2}H_e^{1/2}a_e$.

4.3.1 Large N limit for fermion production

Suppose

$$N \sqrt{\frac{M}{H_e}} \gtrsim 1, \quad (98)$$

which means that the fermion mass is above the Hubble rate at the time of the condensate decay. Clearly, our expansion in $N \sqrt{M/H_e}$ is no longer valid. On the other hand, at large N , the fermion mass remains constant for a long time and we approach a single mass case, which is well understood. In particular,

$$|\beta_k|^2 \simeq 1/2 \text{ for } k \lesssim M^{1/2}H_e^{1/2}a_e, \quad (99)$$

and zero above this cutoff. One expects the transition to the single-mass case to take place at $N^2 M/H_e \sim \mathcal{O}(1)$ and this is indeed what we observe numerically. Fig. 5 displays $|\beta_k|^2$ for three values of N , which correspond to $N \sqrt{M/H_e} = 0.6, 2, 10$. We observe that the curve for $N \sqrt{M/H_e} = 10$ closely resembles that for the single mass (M) case, with the same momentum cutoff $M^{1/2}H_e^{1/2}a_e$.

Hence, as long as $N \sqrt{M/H_e} \gg 1$, we can approximate our system by the single mass case (99).

4.3.2 Upper bound on the abundance of gravitationally produced fermions

In the large N limit corresponding to a long-lived scalar condensate $\langle s \rangle$, we recover the single-mass abundance result,

$$Y_0 \simeq 5 \times 10^{-3} \left(\frac{M}{M_{\text{Pl}}} \right)^{3/2}, \quad (100)$$

where M is the fermion mass generated by the Yukawa coupling to the scalar s , $M = \mathcal{Y}^s \langle s \rangle$. This result applies to $M \ll H_e$, while for heavier fermions, $M \gtrsim H_e$, the abundance is suppressed. Using the PLANCK/BICEP bound $H_e \lesssim 10^{13} \text{ GeV}$ [35, 36], we thus obtain the upper bound on the fermion abundance,

$$Y_{\text{max}} \lesssim 4 \times 10^{-11}. \quad (101)$$

The dark matter abundance is $4.4 \times 10^{-10} \text{ GeV}/M_{\text{DM}}$, hence only fermions heavier than about 10 GeV can play the role of dark matter,

$$M_{\text{DM}} \gtrsim 10 \text{ GeV}, \quad (102)$$

assuming that they are produced via inflation. There are further constraints on such fermions due to the isocurvature perturbations [20].

Note that the late time dynamics of the condensate does not play a role as long as $N \sqrt{\frac{M}{H_e}} \gg 1$. The above bound also applies to the matter dominated Universe since the abundance in this case is further suppressed by $(T_R/M_{\text{Pl}})^\alpha$, with some positive α , as we show in the subsequent section.

Throughout this work, including the above estimate, we have used the “smoothed” scale factor function $a(\eta)$. In reality, $a(\eta)$ contains small oscillations induced by oscillations of the inflaton field after inflation [24]. Their effect is encapsulated by the effective Planck-suppressed operator that couples the inflaton ϕ to the fermion,

$$\mathcal{C} \frac{M}{M_{\text{Pl}}^2} \phi^2 \bar{\Psi} \Psi, \quad (103)$$

where $\mathcal{C} \sim 10^{-1}$. One may estimate particle production via this operator by assuming that M is constant during the inflaton oscillations and $M \ll m_\phi$. The corresponding perturbative production rate has been computed in [12]. Taking the inflaton field value at the beginning of oscillations $\phi_0 \sim M_{\text{Pl}}$ and $M \sim H_e \sim 10^{13} \text{ GeV}$, one finds that this mechanism is somewhat less efficient and the corresponding bound on m_{DM} is in the ballpark of 100 GeV. This shows that fermion production by an oscillating inflaton can be competitive, depending on further details. Note that this effect is due to *classical* gravity.

The above dim-5 operator is also produced by quantum gravity effects [12], although with an unknown coefficient. After inflation, one may use the effective field theory expansion to account for gravity-induced operators [37] and compute their contribution to particle production. The result is that such operators can be very efficient and, thus, the above bound only applies to classical gravity.

4.3.3 Feebly interacting scalar extension

Let us now consider an example of a minimalistic model, where a singlet fermion is produced predominantly by inflation. We identify the fermion with a right-handed neutrino and add one

more degree of freedom [38]: a light real scalar s with the potential

$$V(s) = \frac{1}{2}\mu_s^2 s^2 + \frac{1}{4}\lambda_s s^4, \quad (104)$$

and the coupling to ν_R ,

$$\Delta\mathcal{L} = \frac{1}{2}\mathcal{Y}^s s \nu_R \nu_R + \text{h.c.} \quad (105)$$

The effective right-handed neutrino mass takes on different values at early and late times, as determined by $\langle s \rangle$, while the Dirac neutrino mass is negligible. In addition, ν_R can also have a rigid Majorana mass term contribution, although this plays no significant role. We take the scalar self-coupling to be small, $\lambda_s \ll 1$, and its coupling to the Standard Model, e.g. the Higgs field [39], to be feeble. The self-coupling cannot be arbitrarily small since it is generated at one loop via the fermion loop, hence to avoid fine-tuning, we require

$$\lambda_s > \frac{1}{8\pi^2} |\mathcal{Y}^s|^4. \quad (106)$$

A light scalar field s experiences large quantum fluctuations during inflation. The asymptotic value,

$$\langle s^2 \rangle \rightarrow 0.1 \frac{H^2}{\sqrt{\lambda_s}}, \quad (107)$$

is reached within the characteristic relaxation time $(\sqrt{\lambda_s} H)^{-1}$ [14]. When λ_s is small and the duration of inflation is finite, the field does not have enough time to relax to the asymptotic value. In this case, the field value at the end of inflation is determined primarily by the pre-inflationary initial conditions [23]. The result can then be parametrized in terms of the condensate value at the end of inflation $s_e \equiv \sqrt{\langle s^2(a_e) \rangle}$.

After inflation, the average field s satisfies

$$\ddot{s} + 3H\dot{s} + V'_s = 0.$$

As long as the effective mass is smaller than H , the last term can be neglected such that $\dot{s} \simeq 0$ is a solution to the EOM with the $\dot{s} = 0$ initial condition. Hence, the condensate size remains to be given by s_e for some time after inflation.

The condensate starts oscillating in a quartic potential when the potential term becomes important, i.e. the Hubble rate reduces to

$$H_0 \sim m_s^{\text{eff}} = \sqrt{3\lambda_s} s_e \quad (108)$$

Its contribution to the total energy density is assumed to be subdominant, $V(s) \ll 3H^2 M_{\text{Pl}}^2$. Applying this condition at the start of the oscillation period, we find

$$s_e \ll M_{\text{Pl}}, \quad (109)$$

required for consistency of our analysis. The lower bound $s_e \gtrsim H_e$ is imposed by the scalar fluctuation analysis [23]. The condensate oscillation leads to particle production, i.e. conversion of the zero mode into s -quanta [40, 41]. If the effective neutrino mass is much larger than the effective scalar mass,

$$\mathcal{Y}^s \gg \sqrt{\lambda_s}, \quad (110)$$

the ν_R production from the condensate is highly suppressed kinematically. This is consistent with the radiative stability condition (106) for $\lambda_s \lesssim 1$. Hence, the neutrino production through the condensate decay can be neglected. Similarly, s decay into neutrinos at late times is forbidden as long as the bare mass of ν_R is larger than that of s .

For small enough couplings, s and ν_R do not thermalize, nor is there the freeze-in contribution from the SM thermal bath. Hence, the main contribution to the ν_R abundance comes from gravitational fermion production. It is efficient for $M_\nu = \mathcal{Y}^s s_e \lesssim H_e$ and $N \gg 1$. Specifically, the condensate starts oscillating at $H_0 \simeq H_e/N^2$ which, combined with (108) and $s_e = M_\nu/\mathcal{Y}^s$, requires

$$\frac{M_\nu}{H_e} N^2 \sim \frac{\mathcal{Y}^s}{\sqrt{\lambda_s}} \gg 1, \quad (111)$$

by virtue of (110). This ensures that the condensate is indeed long-lived and the single-mass approximation is adequate.

Ignoring the difference between the Dirac and Majorana fermions, which is within the error bars of our calculation, the ν_R abundance is given by

$$Y_\nu \sim 5 \times 10^{-3} \left(\frac{\mathcal{Y}^s s_e}{M_{\text{Pl}}} \right)^{3/2}, \quad (112)$$

which matches the dark matter abundance for

$$m_\nu \sim 10 \text{ GeV} \times \left(\frac{10^{13} \text{ GeV}}{\mathcal{Y}^s s_e} \right)^{3/2}, \quad (113)$$

with $\mathcal{Y}^s s_e \lesssim H_e \lesssim 10^{13} \text{ GeV}$. The low energy right-handed neutrino mass m_ν is determined by the VEV of the scalar singlet, possibly with the contribution of the rigid mass term. In order to be viable dark matter candidates, these neutrinos must also satisfy the isocurvature constraints, which will be studied elsewhere. Furthermore, \mathcal{Y}^s must be sufficiently small to avoid thermalization of the system¹⁰, while s_e is constrained to be between H_e and M_{Pl} .

The quanta of s do not contribute to the dark matter energy density if they decay into light SM particles after the condensate break-up. This can happen due to higher dimension operators like $s F_{\mu\nu} F^{\mu\nu}$, etc. or a tiny mixing with the Higgs field.

This example shows that inflationary fermion production can be important and even the leading mechanism for production of very weakly interacting particles.

5 Inflation followed by the matter dominated era

The postinflationary dynamics can take place in a matter-dominated background instead of the radiation-dominated one. This is the case for a ϕ^2 local inflaton potential before reheating, which may happen at a much later stage. In the matter dominated epoch ($\eta > 0$),

$$H = H_e \left(\frac{a_e}{a} \right)^{3/2}, \quad a = \frac{1}{4} a_e^3 H_e^2 \left(\eta + \frac{2}{a_e H_e} \right)^2, \quad (114)$$

which connects smoothly to the inflationary regime at $\eta = 0$. We assume that the Universe has the matter-like equation of state, e.g. it is dominated by the non-relativistic inflaton, for an

¹⁰Thermalization of this system was considered in [42, 43], although the results do not apply directly to the case at hand due to a highly non-thermal initial state and $m_\nu \gg m_s$.

extended period such that the boundary conditions in the *out*-region are imposed during this era. Eventually, radiation takes over the energy balance, albeit without affecting the particle number.

Since we are only interested in the *out*-region, in what follows, $u_{A,B}$ will refer to $u_{A,B}^{\text{out}}$. The *in* wavefunctions remain intact.

5.1 Constant mass

At $\eta \gg 1/(a_e H_e)$, the EOM for u_A reads

$$u_A'' + \left(\frac{i}{2} m H_e^2 a_e^3 \eta + \frac{1}{16} m^2 H_e^4 a_e^6 \eta^4 + k^2 \right) u_A = 0 , \quad (115)$$

while the EOM for u_B is obtained by replacing $m \rightarrow -m$. In the $k^2 \rightarrow 0$ limit, the solution can be expressed via hypergeometric functions [44], while in the general case, finding an analytical solution is challenging.

The oscillation frequency at late times is $\omega \simeq am = \frac{1}{4} m H_e^2 a_e^3 \eta^2$ such that the boundary condition at $\eta \rightarrow \infty$ becomes

$$\begin{pmatrix} u_A \\ u_B \end{pmatrix}^{\text{out}} \simeq \begin{pmatrix} 1 \\ \frac{2k}{m H_e^2 a_e^3 \eta^2} \end{pmatrix} \times e^{-\frac{i}{12} m H_e^2 a_e^3 \eta^3} , \quad (116)$$

to linear order in k . Using the inflationary *in* states as before, one computes β_k^2 at $\eta \sim 0$ finding that the effective momentum cut-off for particle production is

$$k_*(m) = m^{1/3} H_e^{2/3} a_e . \quad (117)$$

This corresponds to the momentum at which the three contributions to the frequency become comparable, $m H_e^2 a_e^3 \eta \sim m^2 H_e^4 a_e^6 \eta^4 \sim k^2$. It can also be written as $k_* = a_m m$, where a_m is the scale factor at which $H(a_m) = m$, implying that the produced particles are non- or semi-relativistic at $a = a_m$. Below the cutoff, $|\beta_k|^2$ is approximately 1/2, while above it, the Bogolyubov coefficient goes to zero.

5.2 Step-function mass term

Let us now take the mass term of the form $M \theta(\eta_0 - \eta) + m \theta(\eta - \eta_0)$ with $M \gg m$. Here η_0 corresponds to the Higgs condensate decay time and

$$a_0/a_e = N , \quad (118)$$

as before.

The wave-function at late times is described above, while at $\eta < \eta_0$ it satisfies

$$u_A'' + \left(\frac{i}{2} M H_e^2 a_e^3 \eta + \frac{1}{16} M^2 H_e^4 a_e^6 \eta^4 + k^2 \right) u_A = 0 , \quad (119)$$

with proper boundary conditions at η_0 ,

$$u_A' \Big|_- = u_A' \Big|_+ - i a_0 (M - m) u_A(\eta_0) , \quad (120)$$

The EOM for u_B and the corresponding boundary conditions are obtained by replacing $M, m \rightarrow -M, m$.

The main features of the solution can be understood analytically. At early times, the η^4 term in the EOM is dominated by the linear term in η and can be neglected as long as $M/H_e \times N^{3/2} \ll 1$. Then, the wavefunction satisfies a simple equation at $\eta < \eta_0$,

$$u_A'' + \left(\frac{i}{2} M H_e^2 a_e^3 \eta + k^2 \right) u_A = 0 , \quad (121)$$

whose solution is a linear combination of the Airy functions. The corresponding equation for u_B is obtained by the replacement $M \rightarrow -M$. At small momenta, $k^2 \ll \sqrt{N} M H_e a_e^2$,

$$u_A(\eta) = a_1 \text{Ai} \left(k_*(M) \eta / (2i)^{1/3} \right) + a_2 \text{Bi} \left(k_*(M) \eta / (2i)^{1/3} \right) , \quad (122)$$

$$u_B(\eta) = b_1 \text{Ai} \left(k_*(M) \eta / (-2i)^{1/3} \right) + b_2 \text{Bi} \left(k_*(M) \eta / (-2i)^{1/3} \right) , \quad (123)$$

where $k_*(M)$ is given by (117) with the replacement $m \rightarrow M$, and a_i, b_i are constant coefficients. Since $\eta_0 \simeq \sqrt{N} \eta_e$ and $\eta_e \simeq 2/(a_e H_e)$, the argument of the Airy function is a small number, $k_* \eta \sim \sqrt{N} (M/H_e)^{1/3} \ll 1$. Hence, one can use the expansion

$$\text{Ai}(x) \simeq \frac{1}{3^{2/3} \Gamma(2/3)} (1 + x^3/6) - \frac{x}{3^{1/3} \Gamma(1/3)} , \quad (124)$$

$$\text{Bi}(x) \simeq \frac{1}{3^{1/6} \Gamma(2/3)} (1 + x^3/6) + \frac{3^{1/6} x}{\Gamma(1/3)} . \quad (125)$$

The coefficients a_i and b_i are fixed by the boundary conditions at η_0 .

For momenta below the small-mass cutoff $k_*(m)$, nothing changes compared to the single mass case. We are interested in the higher momenta modes $k \gg k_*(m)$, which bring in new effects. In this case, u_A and u_B are essentially the same at early times, in particular at $\eta_0 + \epsilon$. This is because the corresponding modes should give $\beta_k \simeq 0$ in the single mass case, which implies

$$u_{A,B}(\eta \gtrsim \eta_0) \simeq \frac{1}{\sqrt{2}} e^{-ik\eta} ,$$

with $\omega \simeq k$, neglecting the terms proportional to m . This, together with the derivative jumps (120), determines the boundary condition at η_0 and fixes a_i, b_i .

The Bogolyubov coefficient can be estimated by approximating $u_{A,B}(\eta_e)$ with $u_{A,B}(0)$. We find that the linear and cubic terms in η_0 in the expansion of the Airy functions give contributions of the same order in M/H_e . The universal phase proportional to $k\eta_0$ cancels in $|\beta_k|$ and we get

$$|\beta_k| \simeq \frac{1}{\sqrt{2}} |u_A^{\text{out}}(0) - u_B^{\text{out}}(0)| \sim \frac{M}{H_e} N^{3/2} , \quad (126)$$

in the momentum range $\sqrt{\sqrt{N} M H_e a_e^2} \gg k \gg k_*(m)$. Here we have neglected the logarithmic momentum dependence coming from the *in* states. At higher momenta, the phase attained by $u_{A,B}$ during the evolution from η_0 to η_e becomes universal and the Bogolyubov coefficient gets suppressed by powers of M/k . Thus, the momentum cutoff for the above expression is

$$\tilde{k}_* \simeq N^{1/4} \times M^{1/2} H_e^{1/2} a_e . \quad (127)$$

The resulting fermion abundance is obtained by noting that the particle number is conserved at late times and given by na_R^3 , where a_R is the scale factor at reheating. Since $a_R^3 = a_e^3 H_e^2 / H_R^2$, one finds at $m \ll M$,

$$Y \sim 10^{-2} \times N^{15/4} \frac{M^{7/2} T_R}{H_e^{5/2} M_{\text{Pl}}^2}, \quad (128)$$

where T_R is the reheating temperature. For the matter dominated case, we may take $N \sim 10$ as the benchmark number corresponding to $N = 6$ of the radiation dominated case. The result is suppressed by $T_R / \sqrt{H_e M_{\text{Pl}}} \ll 1$ compared to Y generated during the radiation dominated era.

5.2.1 Universal form

It is interesting to note that the radiation and matter domination results can be put in a *universal form* which involves the Hubble rate at the time of the Higgs condensate decay H_0 instead of N . The Bogolyubov coefficient in both cases has the form $M/H_e \times H_e/H_0$. Hence, we get the universal result

$$|\beta_k| \sim \frac{M}{H_0}, \quad (129)$$

together with the universal cutoff which can be put in the form

$$\tilde{k}_* / a_0 \sim \sqrt{M H_0}. \quad (130)$$

The abundance then reads

$$Y \sim (10^{-3} - 10^{-2}) \times \frac{M^{7/2}}{H_0^2 M_{\text{Pl}}^{3/2}} \times \left(\frac{T_R}{\sqrt{H_0 M_{\text{Pl}}}} \right)^\gamma, \quad (131)$$

where γ is 0 and 1 for the radiation and matter dominated cases, respectively, and the prefactor uncertainty represents the typical “error-bars” expected in our calculation. Note that H_0 is fixed by the effective scalar mass at the end of inflation, $m_{\text{eff}} \sim \sqrt{3\lambda_h} \langle h \rangle$. This expression clearly shows the suppression of Y in the matter dominated case: $\frac{T_R}{\sqrt{H_0 M_{\text{Pl}}}} < 1$ since reheating occurs after the condensate decay by definition.

Similarly, the single mass result ($N \gg 1$) can be put in the universal form,

$$Y_0 \simeq 10^{-2} \left(\frac{M}{M_{\text{Pl}}} \right)^{3/2} \times \left(\frac{T_R}{\sqrt{M M_{\text{Pl}}}} \right)^\gamma, \quad (132)$$

where $\gamma = 0$ or 1, as in (131). Again, $\frac{T_R}{\sqrt{M M_{\text{Pl}}}} < 1$ by assumption of a long matter-dominated period.

The T_R suppression of the abundance is a common feature of particle production in the matter dominated epoch. Indeed, if particle production is dominated by early times,

$$Y \simeq \frac{\text{const}}{T_R^3 a_R^3} \propto H_R^{1/2} \propto T_R.$$

On the other hand, in the radiation domination case, the T_R dependence cancels out. This conclusion also applies to smooth $M(\eta)$ functions, e.g. the thermal mass, hence the particle abundance in the matter dominated case is suppressed compared to that in the radiation dominated scenario.

Given the above universal suppression factor, we conclude that particle production is more efficient in the radiation-dominated background and the particle abundance produced in the matter-dominated case can be made very small by reducing the reheating temperature, which is only bounded by 4 MeV from below [45].

6 Conclusion

We have studied inflationary production of fermions in realistic cosmological settings. The production efficiency is determined by the fermion mass, which is time-dependent and can be very large in the Early Universe. For example, the SM fermion mass is controlled by the Higgs field value. In the absence of significant couplings to the inflaton, scalar fields experience large fluctuations during inflation, which drive the average field value to the Hubble scale and above. Thus, quarks and leptons were many orders of magnitude heavier during inflation, compared to their current masses. This dramatically increases efficiency of their gravitational production.

Using the Bogolyubov coefficient approach, we obtain general results for gravitational production of fermions with sharp and slow mass variations, which we model by a step-function and a thermal mass time dependence. For the sharp mass decrease, the resulting particle abundance scales as

$$Y \propto \frac{M^{7/2}}{M_{\text{Pl}}^{3/2} H_e^2},$$

while the slow mass decrease results in

$$Y \propto \frac{M^3}{(M_{\text{Pl}} H_e)^{3/2}},$$

where M the effective fermion mass shortly after inflation and $H_e \gg M$ is the Hubble rate at the end of inflation. These results assume radiation domination after inflation, while in the case of matter domination, the abundance is suppressed by an additional factor depending on the reheating temperature.

Applying our results to the SM fermions, we find that the production efficiency grows by many orders of magnitude compared to that based on the constant low energy masses. Nevertheless, the energy density of the produced particles remains small and does not affect the standard approach to reheating. However, the production mechanism can be relevant to the scenarios where the inflaton decays entirely into the dark sector states by creating an irreducible SM background. These considerations also apply to production of the right-handed neutrinos with the Higgs Yukawa couplings. Such neutrinos are produced by inflation, via the Higgs condensate decay and through the freeze-in mechanism. We find that gravitational particle production is (at best) subleading in this case.

Inflationary fermion production can also be the leading particle source. For example, if the right-handed neutrinos couple to a light singlet scalar, it induces a large Majorana neutrino mass in the Early Universe. For small enough couplings, the resulting gravitational particle production dwarfs other sources and can account for the dark matter abundance. This scenario is subject to the isocurvature constraints to be studied in a subsequent publication.

We find the following general result: inflationary expansion can be responsible for the fermionic dark matter abundance only if the (low energy) fermion mass is bounded by

$$m_{\text{DM}} \gtrsim 10 \text{ GeV}.$$

This bound assumes a smooth transition from inflation to radiation/matter domination and is based on the Hubble rate constraint $H_e \lesssim 10^{13} \text{ GeV}$. Therefore, *classical* gravity cannot produce a sufficient number of keV-scale sterile neutrinos. In contrast, quantum gravity-induced operators can account for cold, keV sterile neutrino dark matter free of the isocurvature constraints [12].

Acknowledgements. OL acknowledges support from the Magnus Ehrnrooth foundation. The work of FK is supported in part by the National Natural Science Foundation of China under grant No. 12342502.

References

- [1] V. Mukhanov, “Physical Foundations of Cosmology,” Cambridge University Press, 2005; doi:10.1017/CBO9780511790553.
- [2] J. Aalbers *et al.* [LZ], Phys. Rev. Lett. **135**, no.1, 011802 (2025).
- [3] L. Parker, Phys. Rev. **183**, 1057-1068 (1969); A. A. Grib and S. G. Mamaev, Yad. Fiz. **10**, 1276-1281 (1969); Y. B. Zeldovich and A. A. Starobinsky, Zh. Eksp. Teor. Fiz. **61**, 2161-2175 (1971)
- [4] L. Parker, Phys. Rev. D **3**, 346-356 (1971) [erratum: Phys. Rev. D **3**, 2546-2546 (1971)].
- [5] S. G. Mamaev, V. M. Mostepanenko and A. A. Starobinsky, Zh. Eksp. Teor. Fiz. **70**, 1577-1591 (1976); A. A. Grib, S. G. Mamaev and V. M. Mostepanenko, Gen. Rel. Grav. **7**, 535-547 (1976).
- [6] O. Lebedev, JCAP **02**, 032 (2023).
- [7] A. A. Starobinsky, Phys. Lett. B **91** (1980) 99-102.
- [8] A. H. Guth, Phys. Rev. D **23** (1981) 347-356.
- [9] A. D. Linde, Phys. Lett. B **108** (1982) 389-393; Phys. Lett. B **129** (1983), 177-181.
- [10] N. N. Bogolyubov, Sov. Phys. JETP **7**, 41-46 (1958) JINR-R-94.
- [11] D. J. H. Chung, L. L. Everett, H. Yoo and P. Zhou, Phys. Lett. B **712**, 147-154 (2012).
- [12] F. Koutroulis, O. Lebedev and S. Pokorski, JHEP **04**, 027 (2024).
- [13] A. A. Starobinsky, Lect. Notes Phys. **246**, 107-126 (1986).
- [14] A. A. Starobinsky and J. Yokoyama, Phys. Rev. D **50**, 6357-6368 (1994).
- [15] A. Boyarsky, O. Ruchayskiy and M. Shaposhnikov, Ann. Rev. Nucl. Part. Sci. **59**, 191-214 (2009).
- [16] A. Boyarsky, M. Drewes, T. Lasserre, S. Mertens and O. Ruchayskiy, Prog. Part. Nucl. Phys. **104**, 1-45 (2019).
- [17] L. H. Ford, Rept. Prog. Phys. **84**, no.11, 116901 (2021).
- [18] E. W. Kolb and A. J. Long, Rev. Mod. Phys. **96**, no.4, 045005 (2024).
- [19] T. S. Bunch and P. C. W. Davies, Proc. Roy. Soc. Lond. A **360**, 117-134 (1978).
- [20] N. Herring and D. Boyanovsky, Phys. Rev. D **101**, no.12, 123522 (2020).
- [21] J. Klaric, A. Shkerin and G. Vacalis, JCAP **02**, 034 (2023).

[22] B. Barman, S. Cléry, R. T. Co, Y. Mambrini and K. A. Olive, JHEP **12**, 072 (2022).

[23] D. Feiteira and O. Lebedev, doi:10.1088/1475-7516/2025/07/003 [arXiv:2503.14652 [hep-ph]].

[24] Y. Ema, R. Jinno, K. Mukaida and K. Nakayama, JCAP **05**, 038 (2015).

[25] F. L. Bezrukov and M. Shaposhnikov, Phys. Lett. B **659**, 703-706 (2008).

[26] K. Enqvist, S. Nurmi, S. Rusak and D. Weir, JCAP **02**, 057 (2016).

[27] C. Cosme, F. Costa and O. Lebedev, JCAP **06**, 031 (2024).

[28] E. W. Kolb and M. S. Turner, Front. Phys. **69**, 1-547 (1990).

[29] O. Lebedev and A. Westphal, Phys. Lett. B **719**, 415-418 (2013).

[30] M. Laine and A. Vuorinen, “Basics of Thermal Field Theory,” Lect. Notes Phys. **925**, pp.1-281 (2016), Springer, 2016.

[31] K. Ichikawa, T. Suyama, T. Takahashi and M. Yamaguchi, Phys. Rev. D **78**, 063545 (2008).

[32] S. Dodelson and L. M. Widrow, Phys. Rev. Lett. **72**, 17-20 (1994).

[33] L. J. Hall, K. Jedamzik, J. March-Russell and S. M. West, JHEP **03**, 080 (2010).

[34] C. Cosme, F. Costa and O. Lebedev, Phys. Rev. D **109**, no.7, 075038 (2024).

[35] Y. Akrami *et al.* [Planck], Astron. Astrophys. **641**, A10 (2020).

[36] P. A. R. Ade *et al.* [BICEP and Keck], Phys. Rev. Lett. **127**, no.15, 151301 (2021).

[37] O. Lebedev and J. H. Yoon, JCAP **07**, no.07, 001 (2022).

[38] A. Kusenko, Phys. Rev. Lett. **97**, 241301 (2006).

[39] O. Lebedev, Prog. Part. Nucl. Phys. **120**, 103881 (2021).

[40] P. B. Greene, L. Kofman, A. D. Linde and A. A. Starobinsky, Phys. Rev. D **56**, 6175-6192 (1997).

[41] S. Y. Khlebnikov and I. I. Tkachev, Phys. Rev. Lett. **77**, 219-222 (1996).

[42] V. De Romeri, D. Karamitros, O. Lebedev and T. Toma, JHEP **10**, 137 (2020).

[43] O. Lebedev and T. Toma, JHEP **05**, 108 (2023).

[44] Valentin Zaitsev and Andrei Polyanin, “Handbook of Exact Solutions for Ordinary Differential Equations”, Chapman and Hall/CRC, 2002.

[45] S. Hannestad, Phys. Rev. D **70**, 043506 (2004).